SYNTHESIS AND CHARACTERIZATION OF TERPYRIDINE BASED COORDINATION POLYMERS

A Thesis

Submitted to the Graduate Faculty

in Partial Fulfilment of the Requirements

for the Degree of Masters of Science

Molecular and Macromolecular Sciences

Department of Chemistry

Faculty of Science

University of Prince Edward Island

Michael J. Cowper

Charlottetown, Prince Edward Island

March 2017

Abstract

Utilizing a radical-nucleophilic aromatic substitution reaction, a novel bis-terpyridine compound containing a high degree of conjugation was synthesized. This compound was then used along with a series of transition metal compounds to create a series of coordination polymers. The metals used in this series were iron, resulting in a deep purple compound; nickel, resulting in a pale yellow compound; zinc, resulting in a slightly pink, off white compound; cobalt, resulting in a vibrant turquoise compound; copper, resulting in a dark pastel green compound; and ruthenium, resulting in a dark red compound.

The iron coordination polymer was characterized using NMR spectroscopy, and was estimated to possess a molecular weight just under 40,000 g/mol using viscometric analysis. Conductivity measurements were performed on the iron polymer, the results of which unfortunately showed no conductivity. The thermal properties of the iron coordination polymer were also examined, and using TGA it was found to undergo two major decompositions at approximately 460 °C and 485 °C losing 11.27% and 55.04% mass respectively. It was also observed to undergo a glass transition at -37.86 °C.

The full polymer series was examined using NMR spectroscopy, and several of the compounds were also examined using EPR spectroscopy. Several of the polymers were investigated using fluorescence spectroscopy, and the zinc polymer displayed an unexpected fluorescence enhancement of nearly five times over the uncoordinated monomer. Quantum yield experiments determined that this polymer has a quantum yield of 0.33%.

Acknowledgements

First and foremost I would like to thank my supervisors Dr. Alaa Abd-El-Aziz and Dr. Rabin Bissessur. Dr. Abd-El-Aziz has believed in and supported me ever since I started working in his lab in the fourth year of my undergrad, and I wouldn't be where I am now if it were not for him. Dr. Bissessur has been a constant source of support and inspiration ever since my move to the University of Prince Edward Island. I consider it an honour to have been a member of both of their lab groups.

I would also like to thank all of the members of both of the lab groups I have been part of, past and present. I would especially like to thank Jessica Pilfold, both for taking me under her wing and introducing me to the workings of a research lab as well as being a constant source of support and a wonderful friend to this day. Similarly I need to thank all my friends in the department of chemistry, thank you for everything the past few years. I am also very grateful to all the members of the UPEI and UBCO faculty for their assistance and wise words. A special thanks to Stephen Scully for all his assistance throughout the course of my degree.

Thank you to my family for their endless support and encouragement. Particularly to my mother who has always been there for me. Most of all I would like to thank my wonderful girlfriend, Heather Crane, for always being there for me.

Table of Contents

List of Figures

List of Tables

List of Abbreviations and Symbols

°C	degrees Celsius
ε	dielectric constant
[η]	intrinsic viscosity
η_{rel}	relative viscosity
η_{sp}	specific viscosity
λ_{max}	wavelength of maximum fluorescence
c	concentration
cm^{-1}	wavenumbers (infrared spectroscopy)
cps	counts per second
CT	charge transfer
d	doublet (in a spectrum)
ddd	doublet of doublets of doublets (in a spectrum)
DMF	dimethylformamide
DMSO	dimethyl sulfoxide
DPA	9,10-diphenylanthracene

DSC	differential scanning calorimetry
eq.	equivalent
EPR	electronic paramagnetic resonance spectroscopy
g	grams
G	gauss
GPC	gel permeation chromatography
h	hour
^{1}H NMR	proton nuclear magnetic resonance spectroscopy
HPLC	high-performance liquid chromatography
HSQC	heteronuclear single quantum coherence (NMR experiment)
IR	infrared spectroscopy
K	kelvin
NMR	nuclear magnetic resonance spectroscopy
m	multiplet (in a spectrum)
M	molarity
mg	milligrams
mL	millilitres

M_n	number average molecular weight
mmol	millimole
mol	mole
m_s	spin projection quantum number
M_w	weight average molecular weight
PEG 1000	polyethylene glycol (average molecular weight = 1000 g/mol)
PLED	polymer light emitting diode
ppm	parts per million
PPV	poly(p-phenylene vinylene)
s	seconds (with reference to time)
s	singlet (in a spectrum)
S_0	singlet ground electronic energy level
S_1	singlet first excited electronic energy level
$S_{RN}1$	radical-nucleophilic aromatic substitution
T_1	triplet first excited electronic energy level
T_g	glass transition temperature
TGA	thermogravimetric analysis

XRD	powder x-ray diffraction analysis

1 – Introduction

Materials chemistry is a constantly expanding field, and new compounds are continuously being created for a vast range of applications. One exciting branch of this field is that of coordination polymers, with a myriad of potential applications in fields ranging from biomedical to light capture.[1,2] While coordination polymers themselves have a wide range of interesting properties and useful applications, the choice of appropriate organic monomers allows for the addition of conducting properties, with the coordination polymers now acting as molecular wires.

1.1 – Coordination Polymers

1.1.1 – History

The study of coordination polymers is a relatively new field of chemistry, being less than a century old, with the beginning of its rise in popularity not occurring until the 1950s. The earliest known synthetically produced coordination polymer is Prussian blue, with its synthesis first being reported by Stahl in 1731[3], although its structure and identity as a coordination polymer was not known until the advent of x-ray crystallography.[4] This compound has the molecular formula $Fe_4[Fe(CN)_6]_3 \cdot xH_2O$ and exists in a three dimensional lattice consisting of ferricyanide ions coordinating to Fe^{II} metal centres, as can be seen in Figure 1.

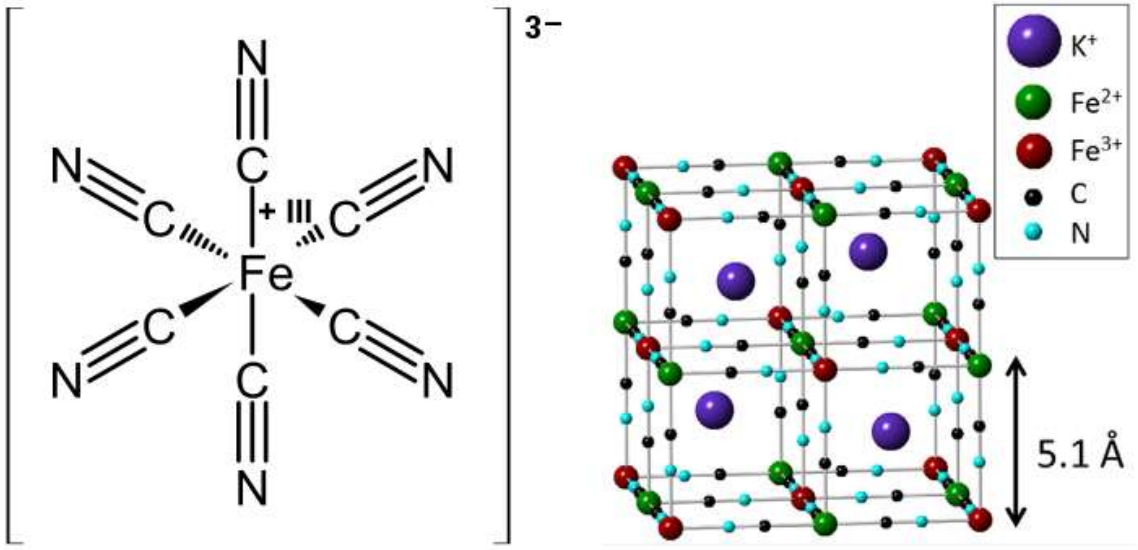

Figure 1 – Ferricyanide ion (left) and structure of Prussian blue including potassium counterions[5] (right).

Two of the earliest intentionally synthesized coordination polymers were silver cyanide, reported in 1935 by West,[6] and nickel rubeanate, reported in 1944 by Jensen,[7] both of which can be seen in Figure 2. The first big boom in coordination polymer research occurred during World War II, funded by the US Air Force with the intention of producing highly thermally stable polymers for use in aerospace applications. Unfortunately this result was never achieved, with most of the polymers being less stable than the monomeric coordination compounds.[8] Interest in coordination polymers fell off

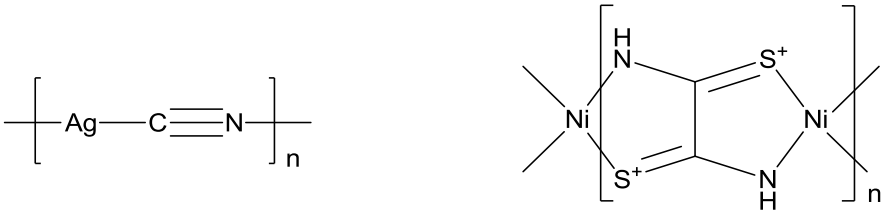

Figure 2 – Silver cyanide (left) and nickel rubeanate (right).

after this, largely due to the difficulty in characterizing these compounds. However, the preparation of ferrocene by Kealy and Paulson in 1951,[9] followed by its structural determination by Wilkinson in 1952,[10] once again sparked interest in coordination polymers, with research truly taking off in the 1970s.

Some of the earliest work in the design of coordination polymers actually belongs to the related field of crystal engineering. The design of supramolecular structures based on the consideration of the geometry and topology of the component molecules was pioneered by A.F. Wells in the 1970s. Wells reduced supramolecular structures to a system of points with specific and known geometries that were then joined to a certain number of other points with specific and known geometries. These connected points of known geometries could then be used to mathematically calculate the overall superstructure.[11,12]

Parallels between this approach to crystal engineering and the design of coordination polymers can easily be drawn, but it was not until the 1990s that the idea was extended to this field by R. Robson.[13] While Wells looked at the problem as a series of inorganic points, Robson adapted the approach to include the combination of inorganic "nodes" and organic "spacers." This approach is the basis for the modern approach to coordination polymer design and led to an explosion of research in the field in the following years.

1.1.2 – Characteristics of Coordination Polymers

There is some disagreement[14-16] over the exact details of such a definition, but a coordination polymer can generally be defined as "a coordination compound with repeating coordination entities extending in 1, 2, or 3 dimensions."[16] These "repeating coordination entities" can vary quite significantly in their makeup, and as a result coordination polymers can be divided into several types based on these coordination entities. These types are: (1) polymerized ligands already coordinated to metals, (2) ligands already in a polymer chain coordinated to metals, and (3) coordination complexes of ligands and metals forming the polymer backbone.[17] The work in this thesis focuses on the third type of coordination polymer, with repeating organic subunits coordinated to metal centres forming the polymer backbone.

One important characteristic of coordination polymers is dimensionality, the ability to exist in 1, 2, or 3 dimensions based upon the coordination number of the metal centres and the denticity of the ligands. For example, the silver cyanide and nickel rubeanate polymers, as can be seen in Figure 2, extend in one dimension while Prussian blue, as can be seen in Figure 1, extends in three dimensions. The dimensionality of a coordination polymer determines the structure it will take. One dimensional coordination polymers will form single chain polymers, two dimensional coordination polymers will form molecular sheets similar in structure to graphene, and three dimensional coordination polymers will form network metal organic frameworks, as can be seen in Figure 3.

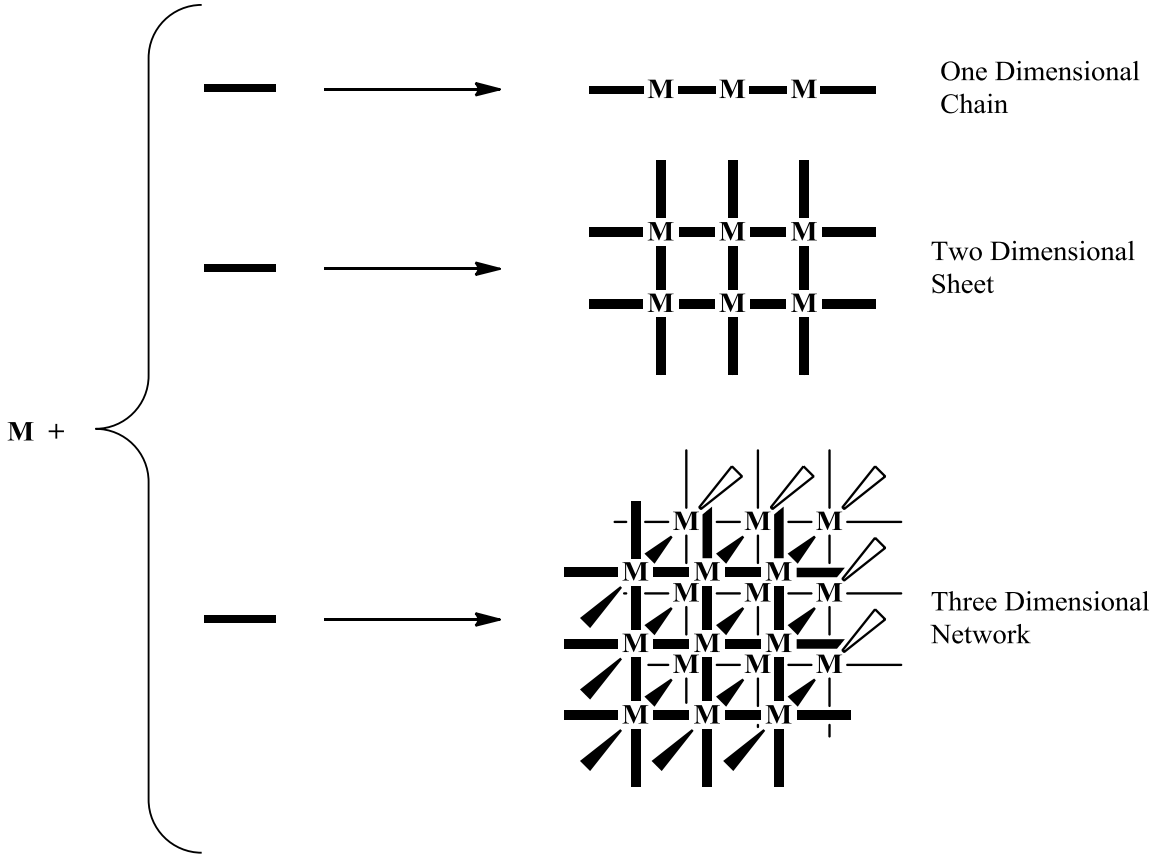

Figure 3 – Dimensionality of coordination polymers.

Coordination polymers possess a number of desirable properties including thermal stability, conductivity, luminescence, porosity, and size- and shape-selective catalytic ability.[18,19] One of the most interesting properties of coordination polymers is their high degree of tunability, which allow for them to be designed for specific applications. And because of their wide range of useful, tuneable properties, coordination polymers have been adopted for a wide range of applications.

1.1.3 – Applications of Coordination Polymers

Because of the vast array of different nodes and spacers that can be used, the expansive range of coordination polymers that can be made is virtually only limited by the imagination; and because of this wide range of possible structures and functionalities, coordination polymers have potential applications in a similarly wide range of fields. These include applications in the biomedical, storage, and catalytic fields, utilization for their sensor and separation capabilities, creation of semiconducting materials, and exploitation of their photophysical properties for use in luminescent and light capture devices.[20-23]

The creation and study of higher dimensional coordination polymers has a high degree of overlap with the field of metal organic frameworks, and as such these coordination polymers share many of the same potential applications. Three dimensional coordination polymers typically display highly porous behaviour, similar to zeolites, and therefore many of their applications focus on the utilization of these pores.[20,22] Through the tuning of pore size and shape, coordination polymer networks can be designed to store specific molecules. This includes use in the field of gas storage, an application for which three dimensional coordination polymers has seen a tremendous amount of attention.[24,25] Inclusion of catalytic sites in these pores allows for size exclusive catalytic activity, with the size of the pores determining the size or shape of compounds that are able to approach the catalytic sites.[21] Alternatively, molecules can be inserted into these pores as a means to protect them. This allows for applications such as drug delivery of unstable compounds.[26]

Three dimensional coordination polymers, along with two dimensional sheet coordination polymers with appropriate functionalization, have potential for selective separation applications. The coordination polymers can be tuned to selectively sequester the desired molecule, either in the pores of three dimensional networks or via the functionalization of lower dimensional polymers.[27] Furthermore, these polymers can simultaneously act as sensors to indicate the successful sequestration of the desired compound. This is due to the fact that coordination polymers contain a metal coordination site, often with chromophore properties. As a result, the successful separation of the desired compound can affect a change in the chromophore properties which will announce the presence of the desired compound, sometimes in means as obvious as a colour change.[28]

The chromophore behaviour of the metal nodes or organic spacers in coordination polymers also has other interesting photophysical applications. One of these is the potential use in photovoltaic materials. For example, a rhenium containing coordination polymer designed by Chan has shown potential for use in light harvesting.[29] Similarly, coordination polymers have a very high potential for the use in luminescent materials. In the past few years, there have been several examples of these materials used for the preparation of polymer light emitting diodes (PLED).[30,31]

1.1.4 – Molecular Wires

As mentioned previously, coordination polymers can exist in 1, 2, or 3 dimensions. Coordination polymers that exhibit conductive properties and exist in one

dimension, either by possessing a low coordination number or the use of ligands with high denticity, are often referred to as molecular wires.[32]

Nanowires were first predicted in 1959 by Richard Feynman[33] as a solution to the problem of miniaturization of computing devices, but it wasn't until recently that research on these substances has been feasible. The term "nanowires" describes a broad range of materials including metallic or crystalline substances that exist in an elongated, wire-like structure with diameters in the nanometer regime. Molecular wires exist as a subset of this class of nanostructures.

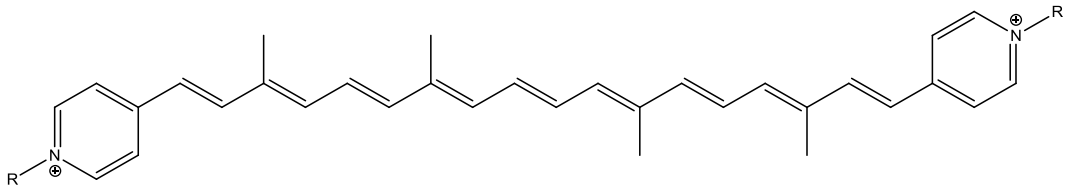

Figure 4 – Carviologen used by Lehn *et al.*[34]

The term "molecular wire" was first used by the 1988 Nobel Prize winner Jean-Marie Lehn to describe his use of carviologen as a "trans-membrane molecular wire."[34] Molecular wires are a distinct subgroup of nanowires as they, as the name implies, are wires of molecular composition as opposed to the broader nanowire category which also includes crystalline or metallic structures.[35] While shorter molecular wires such as the above carviologen exist, the majority of molecular wires are polymeric in nature, consisting of chains of repeating subunits. As nano and molecular wires' original intended use are in small scale electronics, one important feature of such materials is that they are conductive.

Perhaps the most attractive property of molecular wires is that it is easy to alter their properties. The structure of specific molecular wires can be purpose designed and their properties are highly tunable via simple main chain modifications or addition of side chains.[36-38] Conductivity is a property that must be present for a polymer to be considered a molecular wire. While in nanowires this can be achieved simply by the intrinsic metallic properties of metallic nanowires, conductivity is achieved in molecular wires through the presence of extended conjugation. As a result, molecular wires exist primarily as polymers with a high degree of conjugation.

As nanowires were originally envisaged as components used for the miniaturization of computational devices, it should be no surprise that one of their main intended uses is in nanoscale electronics. Along with the use in electronics of individual "wires," the molecular wires behaves similarly to conducting polymers in general, and as such has many of the same applications.

1.2 – Conducting polymers

1.2.1 – History of Conducting Polymers

Polymers are mostly thought of as insulators, and in general, most are. However, there are several classes of polymers that are able to conduct electricity, with the earliest examples in usage nearly one hundred years ago.[39]

The earliest example of a polymer conducting electricity is the utilization of conductively filled polymers to prevent corona discharge.[39] A conductively filled polymer is a nanocomposite comprised of a "traditional" insulating polymer that has

conducting materials added to the polymer matrix. The next form of conducting polymers discovered were charge transfer (CT) polymers discovered by Akumata in 1954.[40] These compounds consist of interactions between electron acceptor and electron donor species that facilitate charge transfer between the two and typically exist as very brittle, mostly crystalline compounds. The third type of conducting polymers are ionically conducting polymers and were first reported by Wright in 1975.[41] These compounds are polymers that have ionically charged groups chemically bound to the polymer chain, thus allowing for electrical conductivity.[42]

While these three groups of compounds are indeed polymers and are able to conduct electricity, it can be argued that they may not truly deserve to be considered a "conducting polymer." The conductively filled and ionic polymers both rely on groups added to the polymer for electrical conductivity, and CT polymers can be argued to be more similar to crystalline materials.

The first example of a polymer conducting electricity through the polymer backbone, a truly intrinsic conductive polymer, was the discovery of conductivity in doped polyacetylene by MacDiarmid, Shirakawa, and Heeger in 1977.[43] Following this discovery, several other stable conducting polymers were quickly reported, including polypyrrole, polyaniline, and polythiophene.[44-46] Since then the field of conducting polymers has expanded by a massive degree, and because of the significance of the discovery and the influence it has had on this new, expanding field, MacDiarmid, Shirakawa, and Heeger were awarded the Nobel Prize in Chemistry in 2000.

1.2.2 – Properties and Applications of Conducting Polymers

As the name implies, the most important property of a conducting polymer is conductivity. Conductivity in polymers can be explained according to band theory, as described by Harrison in 1979.[47] According to band theory, the conductivity of these polymers is a result of electronic structures, referred to as "bands", and the movement of electrons within these structures. These bands can be considered roughly analogous to molecular orbitals in MO theory, with the highest occupied band being the valence band, and the next, unoccupied band being the conductive band. The difference of energy, the "distance," between these two bands is the "band gap," and it is this gap that determines

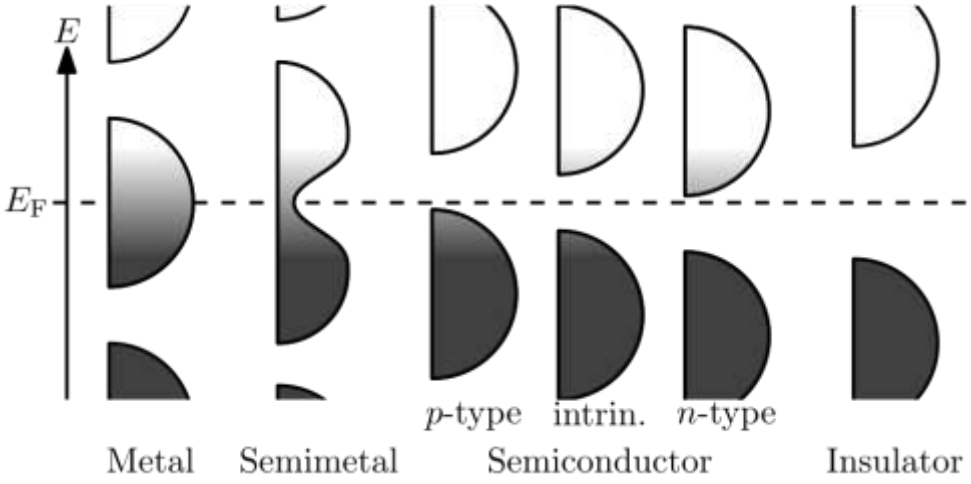

Figure 5 – Energy bands of various types of materials.[48]

a material's conductivity. Metals are highly conductive due to the fact that they possess partially filled energy bands. Semiconductors are materials that have a relatively small band gap, allowing for the promotion of electrons into the conductive band, while the band gap of insulators is large enough that this promotion is impossible.[39,47]

While semiconductors have a band gap narrow enough to facilitate some degree of conductivity, this may be increased by doping the conducting polymers. Conductive polymer doping is the process by which a doping agent is added to either partially oxidize or partially reduce the polymer. Oxidative doping, also known as p-type doping, involves the removal of electrons from the valence band and reductive doping, also known as n-type doping, involves the addition of electrons to the conduction band. Both of these forms of doping result in a change to the structure of the polymer's bands, and as a result increase the conductivity of the material.[49]

One of the most attractive properties of conducting polymers is their tunability. Functional groups can be added to conducting polymers either before or after polymerization, and can be selectively added to alter the properties of the polymer. For example, many polymers are insoluble, but the addition of alkyl groups to the polymer can cause it to be soluble in non-polar solvents, while the addition of ionic groups can result in solubility in polar solvents. As the variety of functional groups is incredibly vast, the ability to alter the properties of a conducting polymer is similarly vast.

Conducting polymers are an incredibly diverse class of compounds, and as such they have applications in a wide range of fields. Because the conductivity of conducting polymers is a result of the delocalization of electrons through an extended conjugation system, many conducting polymers have interesting and useful optical properties. One example of this is the use of conducting polymers in polymer light emitting diodes (PLEDs). These materials were born from the discovery of electroluminescent properties in poly(p-phenylene vinylene) (PPV) by Friend *et al*. in 1990.[50] The addition of light harvesting materials to conducting polymers also allows for their use as organic

photovoltaic materials, with the first example being reported by Heeger in 1995.[51] These are just a couple of examples of the applications of conducting polymers, and many more exist, including usage in electronic and sensing devices, as well as corrosion protection materials.[39]

1.3 – Terpyridine

1.3.1 – Structure and History of Terpyridine

Terpyridine is a molecule that consists of three joined pyridine rings, and while there are many possible substitution patterns, the general term "terpyridine" almost exclusively refers to 2,2`:6`,2``-terpyridine, the structure of which can be seen in Figure 6. Consequently, whenever used in this thesis, "terpyridine" refers to this compound or its derivatives. As a result of the 2,2`:6`,2`` substitution pattern, terpyridine acts as a tridentate chelating ligand, almost like a molecular "claw", and forms stable coordination complexes with many transition metals.

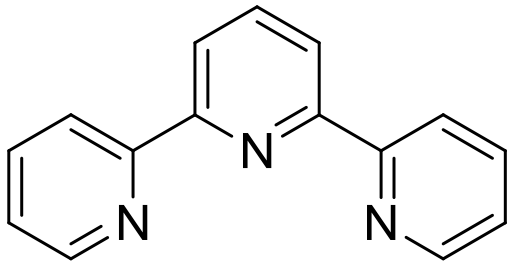

Figure 6 – The structure of 2,2`:6`,2``-terpyridine.

Terpyridine was first synthesized by Morgan and Burstall in 1932, albeit entirely by accident. Morgan and Burstall had been attempting, successfully, to produce large quantities of 2,2`-bipyridine by direct dehydrogenation and isolated terpyridine as one of 20 by-products. Although they did little more with the terpyridine than identify it, they noted its potential usefulness as a ligand for coordination complexes.[52] It was not until several years later that a higher yield, synthetic approach to terpyridine preparation was reported, utilizing a Kröhnke condensation reaction.[53] Interest in the use of terpyridine for metal complexation saw a huge increase in the late 20th century as a result of the strong, distorted octahedral coordination complexes it forms largely championed by Constable[54-57] and Schubert.[58-60]

Also as a result of the strong coordination complexes terpyridine forms with transition metals it has seen use in coordination polymers, with some early examples dating to the early 1990s.[61,62] A significant amount of terpyridine's application in coordination polymers has been to attach metal complexes pendantly to a polymer chain, often as chromophores.[63,64] It has however also been used as the ligands in backbone metal coordination polymers.[65-67]

1.4 – Characterization Techniques

1.4.1 – Nuclear Magnetic Resonance and Electron Paramagnetic Resonance Spectroscopy

Nuclear magnetic resonance (NMR) spectroscopy is one of the most useful techniques in chemistry. While a great deal of information can be discovered using NMR, the most commonly obtained is structural information about a compound. To

provide in depth background and operational details on this form of spectroscopy would be outside the scope of this thesis, and so a brief introduction will be presented.

NMR operates by exposing a compound to a strong magnetic field, which causes the spin states of the nuclei to become non-degenerate, splitting into higher and lower energy states. Whereas before there was an even population between these spin states, there is now an increased population in the lower energy spin state. As a result of the now present energy gap between spin states, nuclei can now absorb electromagnetic radiation, for NMR in the radio wavelength region, and become excited to the higher energy spin state, followed by a relaxation to the lower energy spin state.[68]

The frequency at which nuclei will absorb varies, and is a result of the electronic environment of the nucleus. This shift in frequency is known as the chemical shift of the nucleus and is reported in units of parts per million (ppm). Because this shift is caused by the electronic environment of the nucleus, structural information about the region of the molecule that the nucleus is in can be deduced. In ^{1}H NMR, the integrated area under the signal of a specific proton is dependent on the number of nuclei in identical electronic environments. As a result, the integration of each signal in an NMR spectrum relative to the other signals provides structural information.

Another piece of structural information that can be obtained via NMR spectroscopy comes from the splitting patterns of signals caused by spin-spin coupling. In this process, a nearby chemically bound nucleus will influence the frequency of another nucleus, resulting in the splitting of the signal into a multiplet. In ^{1}H NMR, this

splitting provides information due to the fact that the multiplicity of the signal is directly related to the number of nearby proton nuclei.[68,69]

Electron paramagnetic resonance (EPR) spectroscopy is an analogous technique that looks at electrons instead of nuclei. While it also involves the use of a magnetic field and electromagnetic radiation, it is instead the magnetic field that is varied while the radiation, in the microwave region, is held constant. In EPR it is the electron's magnetic moment (m_s) that is split in energy. As a set of paired electrons will occupy both of these energy levels, an electron must be unpaired in order to absorb electromagnetic radiation and be promoted into the higher energy level. As a result of this, only molecules with unpaired electrons, such as radicals or transition metal complexes with an uneven number of d-electrons, can be analysed using EPR.[70]

While EPR may be less useful than NMR for the structural elucidation of a compound, it can provide important electronic information about the molecule. For example, an electron's g-factor is a result of the applied magnetic field as well as the magnetic fields caused by nuclei in the compound, and can provide information about the atomic or molecular orbital occupied by the electron. EPR is also an extremely effective technique to detect the presence of radicals, and as such is often used in many scientific fields.[71,72]

1.4.2 – Thermal Analysis

When considering potential applications of a compound, information about the compound's thermal properties is very useful. The thermal stability of a compound is very important for determining what applications it may be appropriate for, and can be determined using thermogravimetric analysis (TGA). Differential scanning calorimetry (DSC) is another technique for analyzing a compound's thermal properties and can determine properties such as phase transitions.

TGA is a relatively straightforward technique, and involves heating a sample and measuring its mass during this process. This technique is designed to be sensitive to minute changes in a sample's mass, and as such a balance of high accuracy, typically down to the microgram regime, is required. The TGA instrument will also consist of a furnace that has a high degree of control over heating rate. The thermograms produced via TGA will contain a plot of weight percentage as a function of temperature, and losses of mass will correspond to decompositions of the sample being analysed.[73]

While thermogravimetric analysis covers a wide range of temperatures extending up from room temperature, differential scanning calorimetry covers a wide range of temperatures centred around room temperature. Because the temperature range the DSC can observe extends far below 0°C, the system must either contain a powerful refrigeration unit or utilize a cryogenic fluid such as liquid nitrogen. DSC operates by examining the heat capacity of a compound, and does this by recording the amount of heat required to increase the temperature of the compound as a function of temperature. This rate will experience an abrupt change when the compound experiences a thermal

event, which allows DSC to determine phase changes, such as melting or crystallization, or other thermal properties such as the point of denaturation of proteins.

When examining a polymer, one of the most important thermal properties that can be investigated using DSC is the polymer's glass transition temperature. A glass transition point is the temperature at which a polymer transitions from one state to another. Below this temperature a polymer will exist as a brittle, glassy material, and above it the polymer will be amorphous and "rubbery." Like thermal stability, this is an important property to consider when determining appropriate polymers for a specific application.[74]

1.4.3 – Fluorescent Analysis

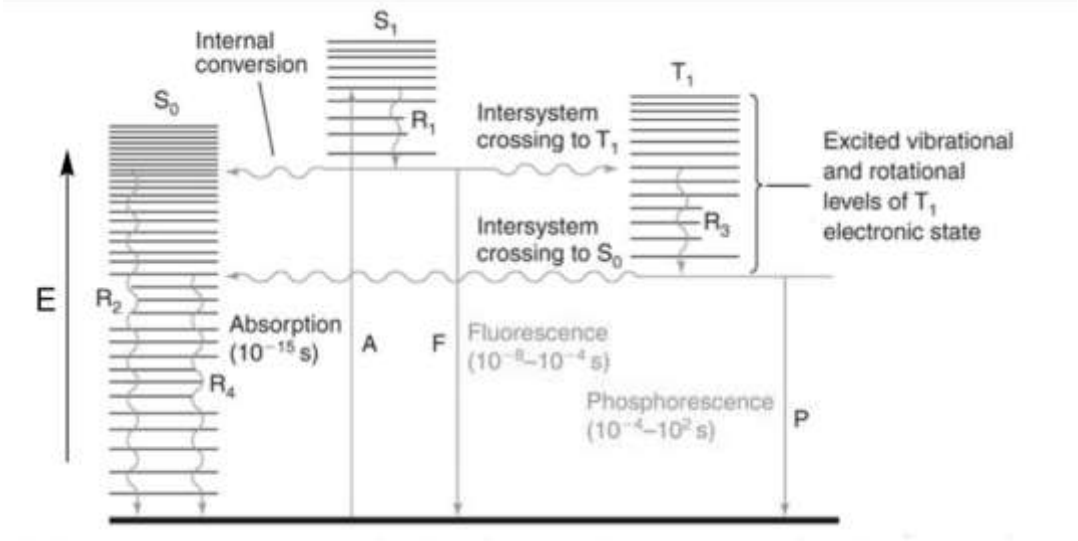

Figure 7 – The Jablonksi diagram.[75]

Photoluminescence occurs when a molecule in an excited electronic state relaxes to its ground state. Fluorescence is one of the two methods through which this relaxation can occur, along with phosphorescence. These processes are best described via the Jablonski diagram, as pictured in Figure 7. The first step in this process is the absorption of a photon. This causes excitation of an electron from the singlet ground energy state (S_0) to an excited energy level of the singlet excited energy state (S_1). From this excited state there are several pathways through which the molecule can relax to the ground electronic energy level.

The first pathway is through an internal conversion, crossing back to a higher vibrational level in the singlet ground state, after which the molecule can relax

vibrationally (R_2 in Figure 7), for example through collisions with other molecules. The second pathway is intersystem crossing from the singlet excited energy state to an excited vibrational level of the excited triplet electronic state. The molecule then undergoes vibrational relaxation in this energy state before relaxing to the S_0 ground energy level through the phosphorescent emission of a photon (P in Figure 7). Fluorescence is the final method of relaxation and involves vibrational relaxation in the S_1 excited state followed by a relaxation to the S_0 ground state through the fluorescent release of a photon (F in Figure 7).[76]

Fluorescence spectroscopy, or fluorimetry, is the spectroscopic technique that measures fluorescent emissions. In it, an electron in a molecule is promoted to an excited energy state through exposure to electromagnetic radiation, often in the ultraviolet or visible range of the spectrum. The molecule is then allowed to relax to the ground energy level, and the energy of the emitted photon is recorded. There are two main fluorescent techniques, excitation fluorimetry and emission fluorimetry. In excitation fluorimetry, a specific wavelength of fluorescent light is monitored while the molecule is exposed to a range of light wavelengths. Conversely, in emission fluorimetry the molecule is excited by a constant wavelength of light while the fluorescent emission over a range of wavelengths is recorded.

Fluorescence spectroscopy is a powerful technique in the field of chemistry. It can be used to quantitatively analyse the presence of a specific analyte in solution, and fluorescent detectors are often used in high pressure liquid chromatography (HPLC). Fluorescence spectroscopy is also a useful tool in the analysis of organic compounds, directly revealing information about the energy levels of compounds.[77]

1.4.4 – Viscometry

One of the most defining properties of any polymeric material is the molecular weight of the compound, often defined as the number average molecular weight (M_n) or the weight average molecular weight (M_w). This property is essentially a measurement of the length of the polymer, dependent on the number of repeating subunits it is comprised of. The ideal technique to determine this property is gel permeation chromatography (GPC), a form of size exclusion chromatography that separates compounds based on their sizes.

Unfortunately, compounds that possess a low solubility or contain cationic metal moieties, both of which are present in the compounds described in this thesis, are either impractical or impossible to analyse using GPC. Compounds must be in solution for GPC to be run, so low solubility makes this difficult, and the presence of cationic metals in the polymer will damage the GPC column. And so, with GPC unavailable, other avenues must be pursued in order to examine the molecular weight of the polymers.

One of these alternative techniques, and the one chosen for use in this thesis, is viscometry. Viscometry measures the viscosity of a solution, and by comparing the viscosity of an unknown compound with that of a model standard, the relative viscosity can supply information about the unknown compound. Unlike GPC, viscometry cannot supply highly precise quantitative results, but it can offer insight into the nature of the material, suggesting a relative molecular weight and providing evidence that a compound exists as a polymer as opposed to a series of oligomers.

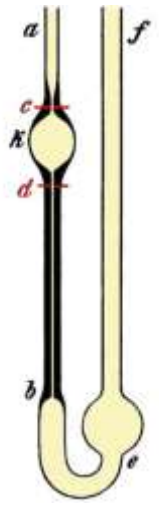

Figure 8 – Ostwald viscometer.

Several different types of viscometers exist, but the one used in this thesis was an Ostwald viscometer, pictured in Figure 8. This type of viscometer consists of a glass tube with a u-bend in it. One arm of the tube has a thin capillary running most of its length, with a reservoir at the bottom and a second reservoir of specific volume at the top. A solution of known concentration is placed in the lower reservoir through the arm without the capillary, and is then drawn up through the capillary until the reservoir with a specific volume is filled. The solution is then timed as it is allowed to flow through the capillary, and the time taken to do so can be used to calculate the kinematic viscosity. This viscosity is then compared with that of a model standard to infer information about the compound. Perhaps most importantly, this technique can be used to determine a polymer's intrinsic viscosity, which can then be used to approximate the polymer's molecular weight by applying the Mark-Houwink equation:[78]

$$[\eta] = KM^a \qquad \textbf{(1)}$$

where [η] is the intrinsic viscosity, M is the molecular weight of the polymer, and K and a are variables related to the polymer-solvent system and the polymer's flexibility respectively.

1.4.5 – XRD and IR

Powder X-Ray Diffraction (XRD) is a technique that uses a directed beam of x-rays and measures the intensity of the diffraction of the beam off a sample through a range of angles. As the name implies, powder XRD requires that a sample be ground into a fine powder to be analysed, and is prepared by being pressed flat either into a recessed sample holder or onto a piece of double sided tape on a glass slide. XRD is most useful in analyzing either crystalline or layered materials. Every crystalline compound has a unique XRD diffractogram, and XRD is commonly used in the analysis of pharmaceutical compounds. With polymers, XRD is helpful in understanding the nature of the polymer, whether it is amorphous or crystalline, and if it is crystalline, to what degree.

Infrared (IR) spectroscopy is a spectroscopic technique that examines either the absorbance or transmittance of infrared radiation as it passes through a sample. The energy of infrared radiation corresponds to frequencies that are resonant with the vibrational modes of molecular bonds. As infrared light passes through a sample, specific frequencies of radiation will be absorbed corresponding to the vibrational energies of the bonds in that sample. As a result, infrared spectroscopy is a useful

technique for examining the structure of a compound, as it will highlight specific functional groups and bond types in that compound.[68]

1.5 – Project Objectives

The purpose of this project is to develop a novel series of highly conjugated coordination polymers, which will ideally possess conductivity. This will be done by preparing a novel organic monomer that both possesses a high degree of conjugation, through the inclusion of aromatic groups and thioethers, and contains two strongly coordinating terpyridine ligands. This monomer will then be used in a coordination reaction with iron chloride in order to produce an iron coordination polymer. This iron coordination polymer will be characterised using several techniques including NMR spectroscopy and viscometry. Its thermal properties will also be investigated using TGA and DSC.

The terpyridine based monomer will then be reacted with several other transition metals to form a coordination polymer series. This series will then be investigated using NMR spectroscopy as well as EPR spectroscopy. The fluorescent properties of the polymer series will also be examined.

2 – Synthesis and Characterization of Iron Coordination Polymer

2.1 – Synthesis of Terpyridine Based Monomer

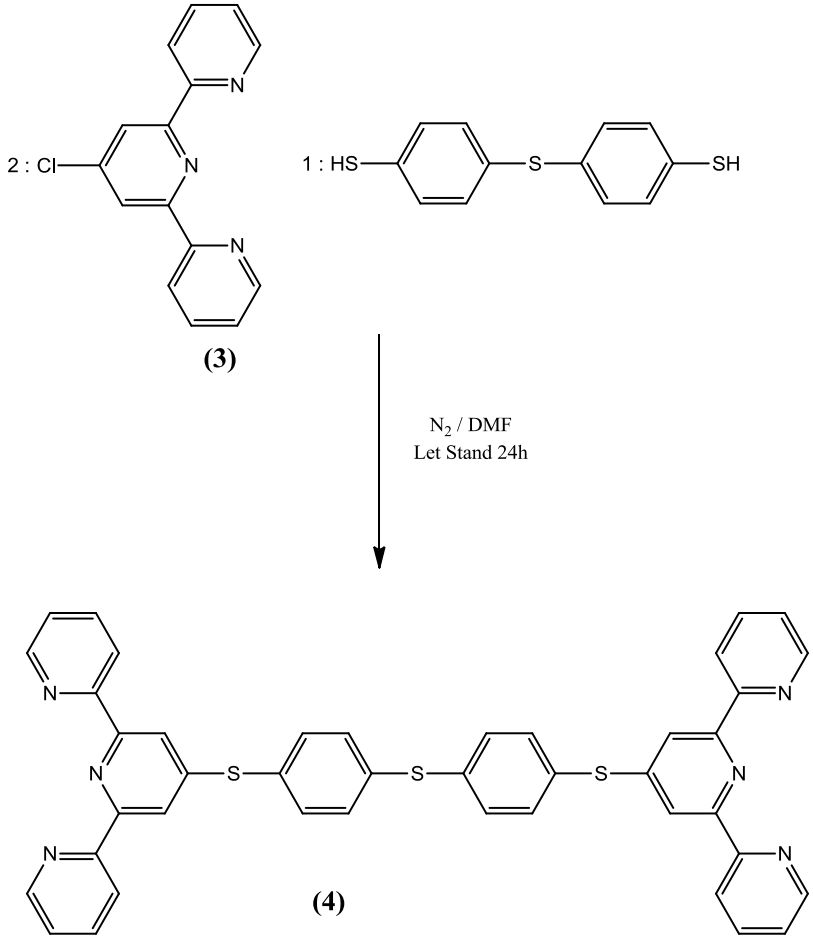

Figure 9 – Synthesis of disubstituted thiobisbenzenethiol-terpyridine monomer by an aromatic $S_{RN}1$ reaction. Compound 3 was prepared according to literature methods.[54]

At first glance, the reaction for the synthesis of the bis-terpyridine-substituted monomer appears quite simple, but while the conditions certainly are, the reasoning behind these conditions is less so. The synthesis was derived from previously reported

methods,[79] and similar reactions have been reported in the literature.[80-82] However, the actual mechanism of this reaction is rarely discussed in great detail, with most publications briefly mentioning the type of reaction this is (an aromatic $S_{RN}1$) and then referencing earlier papers[83-85] without discussing the most notable oddity of this reaction: the absence of stirring. This pattern continues back to the earliest article reporting the aromatic $S_{RN}1$ reaction.[86]

This earliest publication of the aromatic $S_{RN}1$ reaction by Bunnett[86] discusses the large range of applications of the newly described reaction based on earlier work in his lab as well as the investigations of aliphatic radical mediated S_N1 reactions by Kornblum.[87] As the name implies, this reaction is a nucleophilic substitution following a radical chain mechanism with aromatic reactants, one of which must be an aromatic halide. While many aromatic systems undergoing this mechanism require initiation of the radical chain reaction by either photostimulation or the addition of solvated electrons via alkali metals,[86] some systems, such as this reaction's thiophenol and aryl chloride, will auto initiate.

While these aspects are discussed in detail by Bunnett,[86] the explanation as to why stirring is not only not required but will actually disrupt the reaction is not discussed. And while the exact reason is not known, it is likely that stirring will actually serve to quench the radical chain reaction. As the reaction progresses, "pockets of reactivity" are continually forming in which radicals are being formed and radical chain reactions are occurring. Stirring serves to disrupt these "pockets," bringing radicals together, and thereby terminating the chain reaction prematurely. As a result, the absence of stirring would be required for the reaction to go to completion in an appropriate length of time.

2.2 NMR Analysis of Monomer

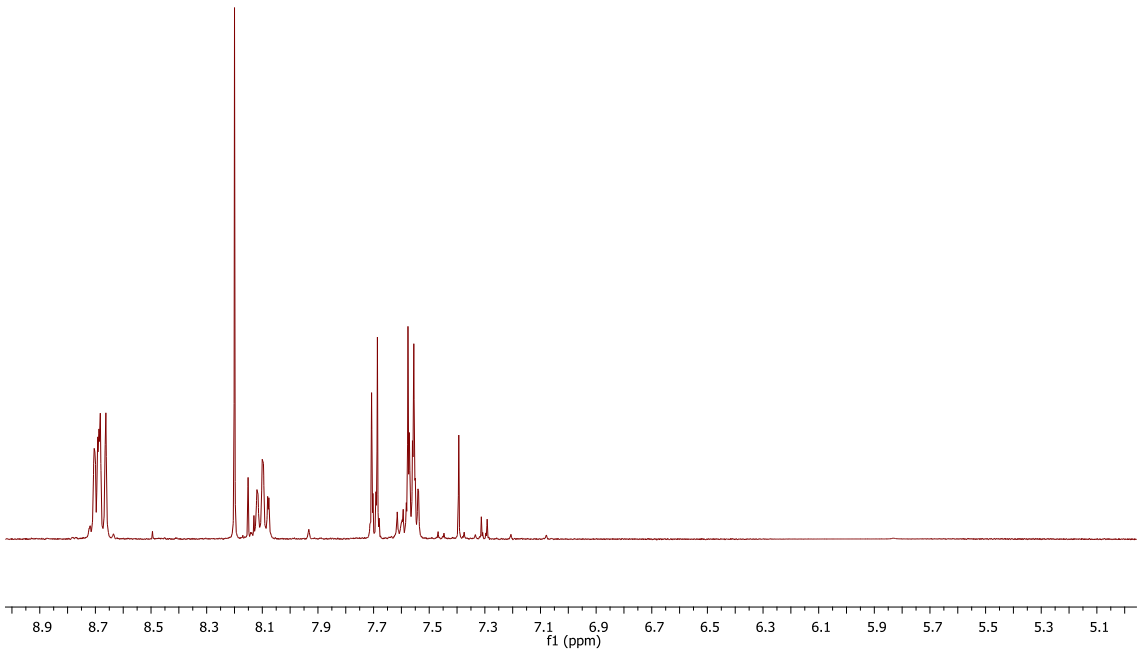

Figure 10 – ^{1}H NMR spectrum of bis-terpyridine monomer.

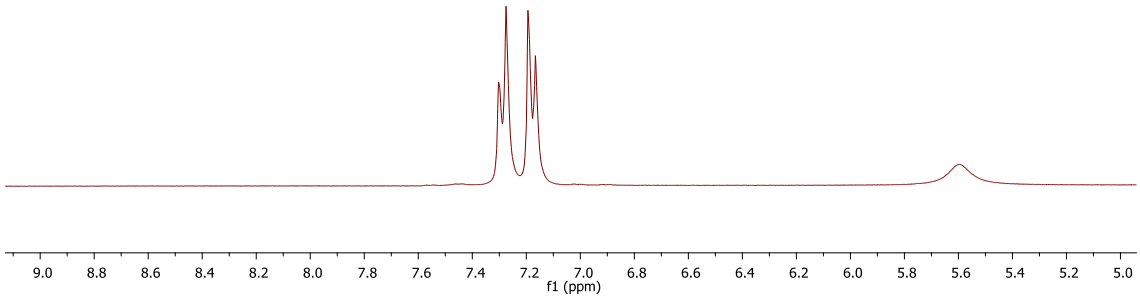

Figure 11 – ^{1}H NMR spectrum of thiobisbenzenethiol.

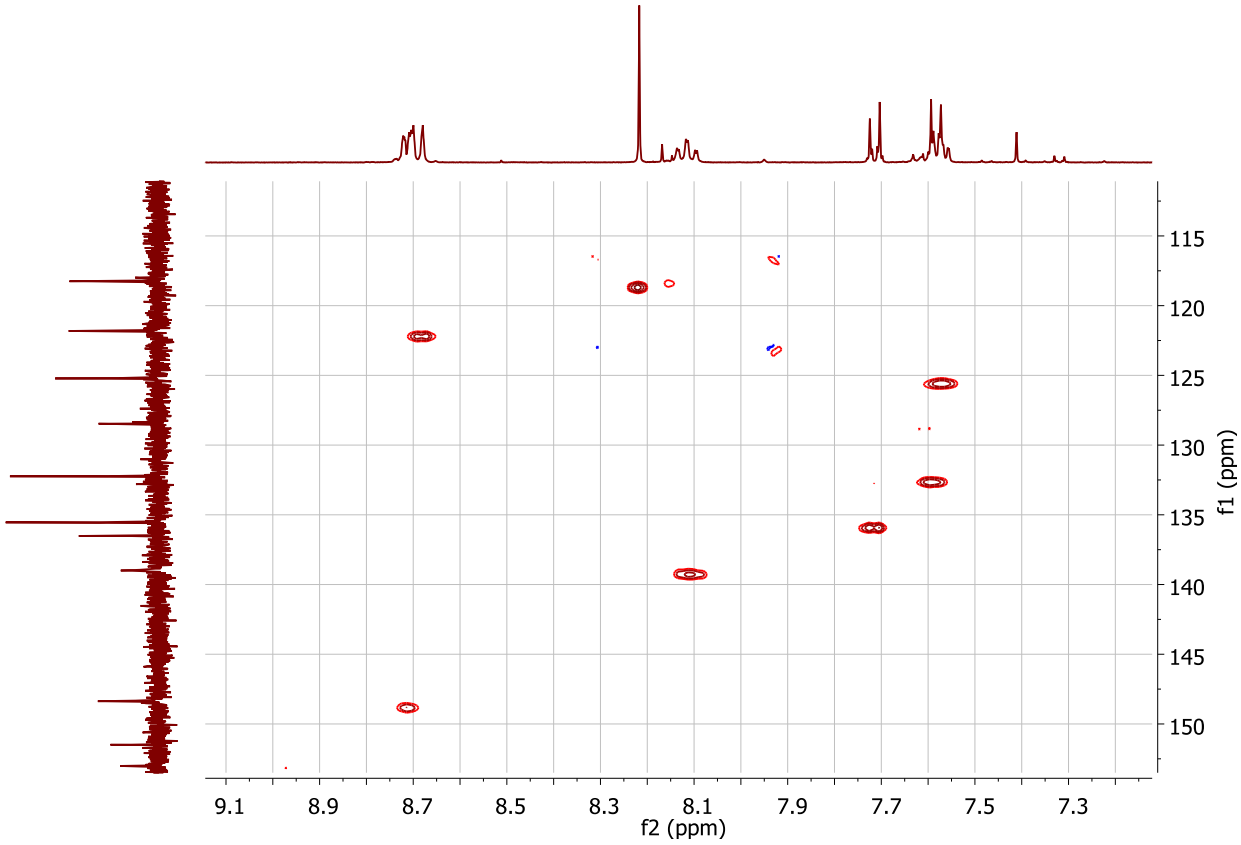

Figure 12 – HSQC spectrum of bis-terpyridine monomer.

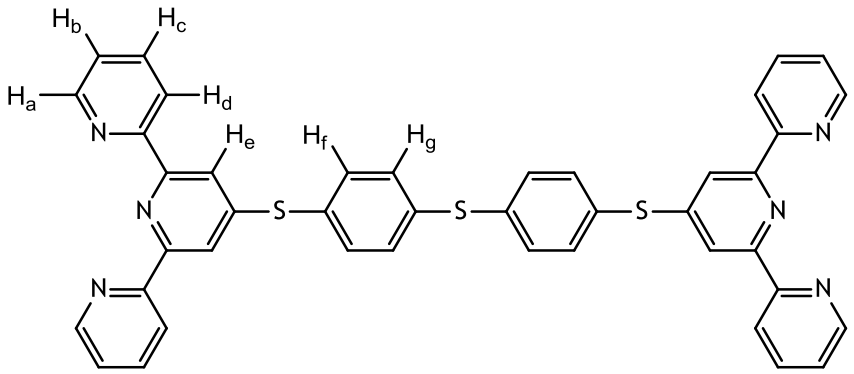

Proton	Shift (ppm)	Multiplicity	Integration
H_a / H_d	8.66-8.75	m	8
H_b / H_g	7.55	m	8
H_c	8.12	ddd	4
H_e	8.22	s	4
H_f	7.72	d	4

Figure 13 – ^{1}H NMR proton assignments for monomer.

The assignments of the ^{1}H NMR signals caused by H_a through H_e are based upon previous investigations of terpyridine[88] and do not differ significantly from those seen in the starting material, 4`-chloro-2,2`:6`,2``-terpyridine. The four signals caused by H_a to H_d appear in the expected locations, and the signal caused by H_e appears as the expected singlet with only a slight shift. The signals resulting from H_f and H_g however do see a significant change from the starting material. In the ^{1}H NMR spectrum of

thiobisbenzenethiol, these two hydrogens appear as two doublets at 7.18 and 7.29 ppm, as can be seen in Figure 11. Following the reaction with terpyridine, these signals have shifted further downfield to 7.57 and 7.70 ppm, with the distance between them increasing, as can be seen in Figure 10. This is due to the fact that the aromatic terpyridine groups serve to further deshield the thiobisbenzenethiol protons. Even more apparent is the disappearance of the thiol proton of the unreacted thiobisbenzenethiol as can be seen in Figure 11 at 5.59 ppm.

The HSQC spectrum of this compound (Figure 12) shows the presence of seven hydrogens bonded to seven unique carbons as well as the presence of five more quaternary carbons. The HSQC spectrum also confirms the assignment of the two multiplet signals as being caused by overlapping signals.

2.3 – Synthesis of Iron Coordination Polymer

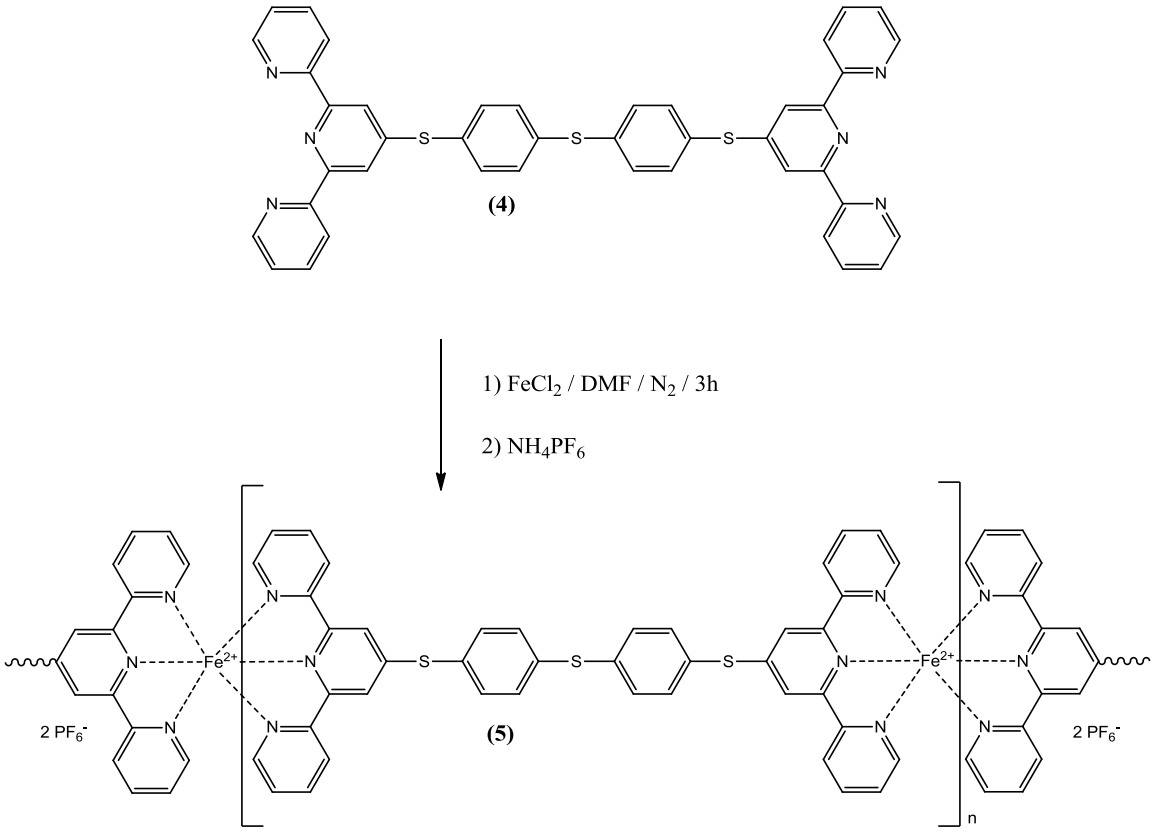

Figure 14 – Synthesis of iron polymer.

The formation of the iron coordination polymer takes place through the coordination reaction of one equivalent of the bis-terpyridine-substituted monomer with one equivalent of iron(II) chloride. The monomer and the coordinated polymer both suffer from very low solubility in most solvents, and as such, the coordination reaction occurs in a minimum volume of DMF as determined by adding solvent dropwise until all reactants have dissolved. The ability for terpyridine to form a coordination complex with

iron is so great that upon the addition of the first drop of solvent, a dark purple colour is immediately present. The reaction solution is then stirred for 3 hours under a nitrogen atmosphere to ensure maximum coordination.

After the reaction is complete, an excess of ammonium hexafluorophosphate is added to the now deep purple solution. This serves to replace the Fe^{2+} metal centre's Cl^- counter ions with the strongly non-coordinating PF_6^- anion. The product is then precipitated by dropwise addition into diethyl ether and isolated via vacuum filtration as a purple powder.

2.4 – Characterization of Iron Coordination Polymer

2.4.1 – NMR Analysis of Polymer

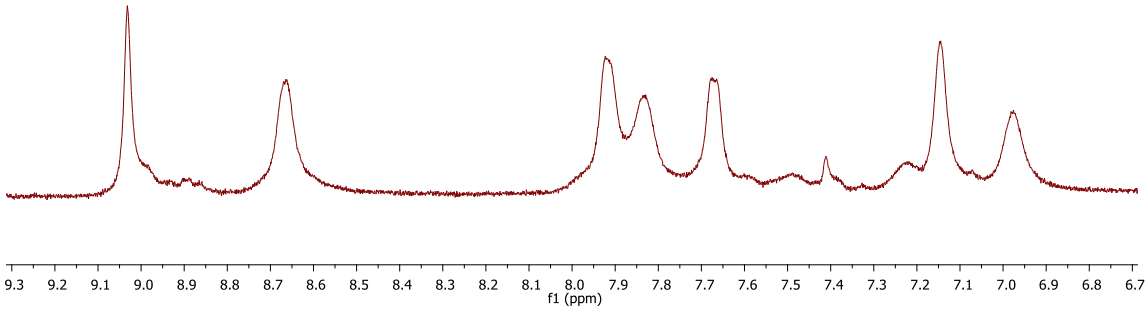

Figure 15 – ^{1}H NMR spectrum of iron coordination polymer.

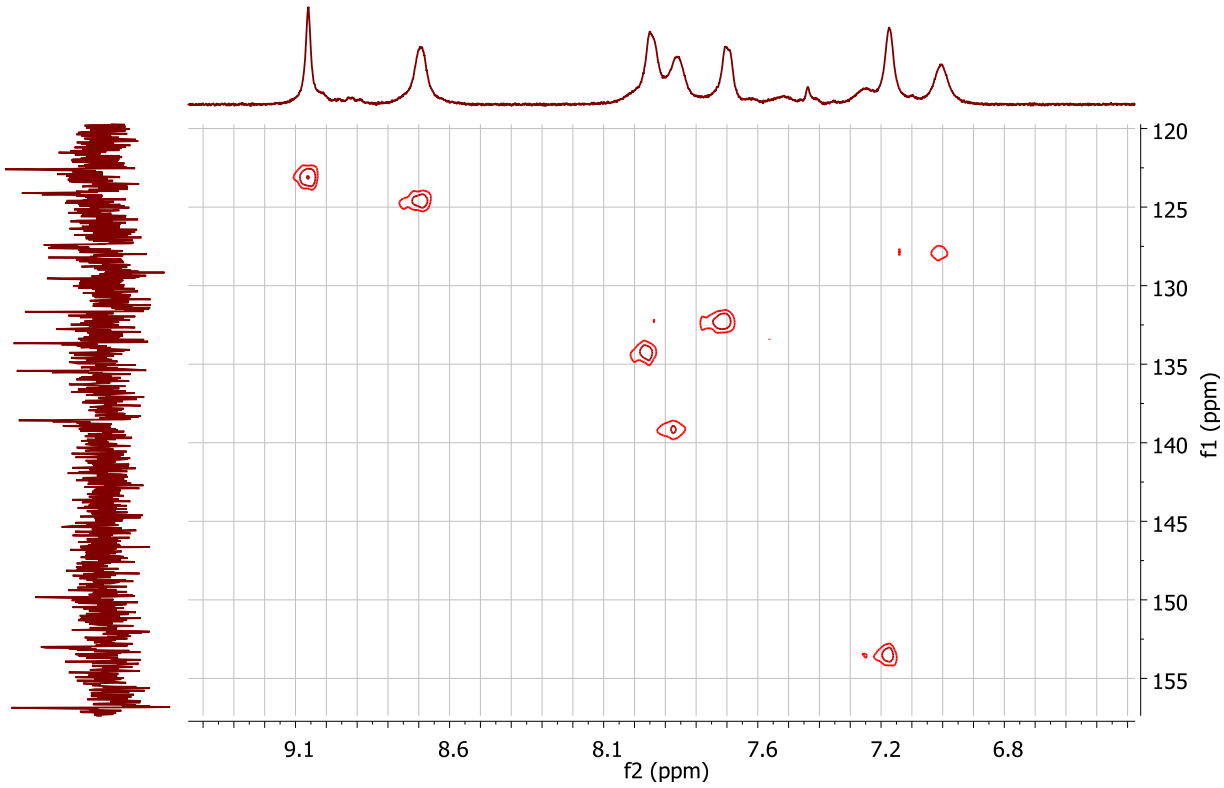

Figure 16 – HSQC spectrum of iron coordination polymer.

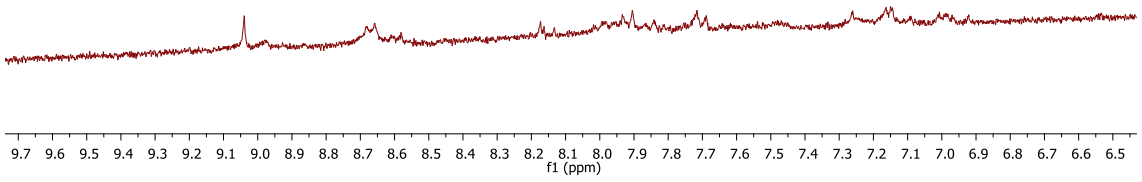

Figure 17 – ^{1}H NMR spectrum of iron coordination polymer obtained at extremely low concentrations.

After the coordination reaction forming the polymer, the ^{1}H NMR spectrum shows a broadening of all of the signals as can be seen in Figure 15. It was first suspected that this broadening was the result of the polymeric nature of the compound, as large molecular weight compounds experience a reduction in the speed of tumbling on the NMR timescale. However, the molecular weight was determined to be approximately 40,000 g/mol using viscometry (Section 2.4.2), and while this still means the coordination species is a polymer, it is a relatively low molecular weight polymer and therefore this is not likely to be the reason for the peak broadening. To investigate the cause for the peak broadening, a ^{1}H NMR spectrum of the iron coordination polymer was

obtained at extremely low concentrations, as can be seen in Figure 16. For perspective of the concentration, the spectrum in Figure 16 was obtained from 1024 scans, with the signals just visible amongst the noise, and yet, while the signals are more defined than those in Figure 15, they still exhibit peak broadening when compared to the uncoordinated monomer (Figure 10). This indicates that concentration effects are partly responsible for the peak broadening, but not entirely.

A major cause of peak broadening in NMR is paramagnetic effects, but EPR investigation of the iron coordination polymer (Figures 38 and 39) show that there is no paramagnetic behaviour in the polymer, even at low temperatures. Some of the broadening effect may be caused by π-stacking interactions between the polymer chains, but because this is not evident in the spectrum of the pure monomer, it is likely that some of the peak broadening is due to the compound's polymeric nature.

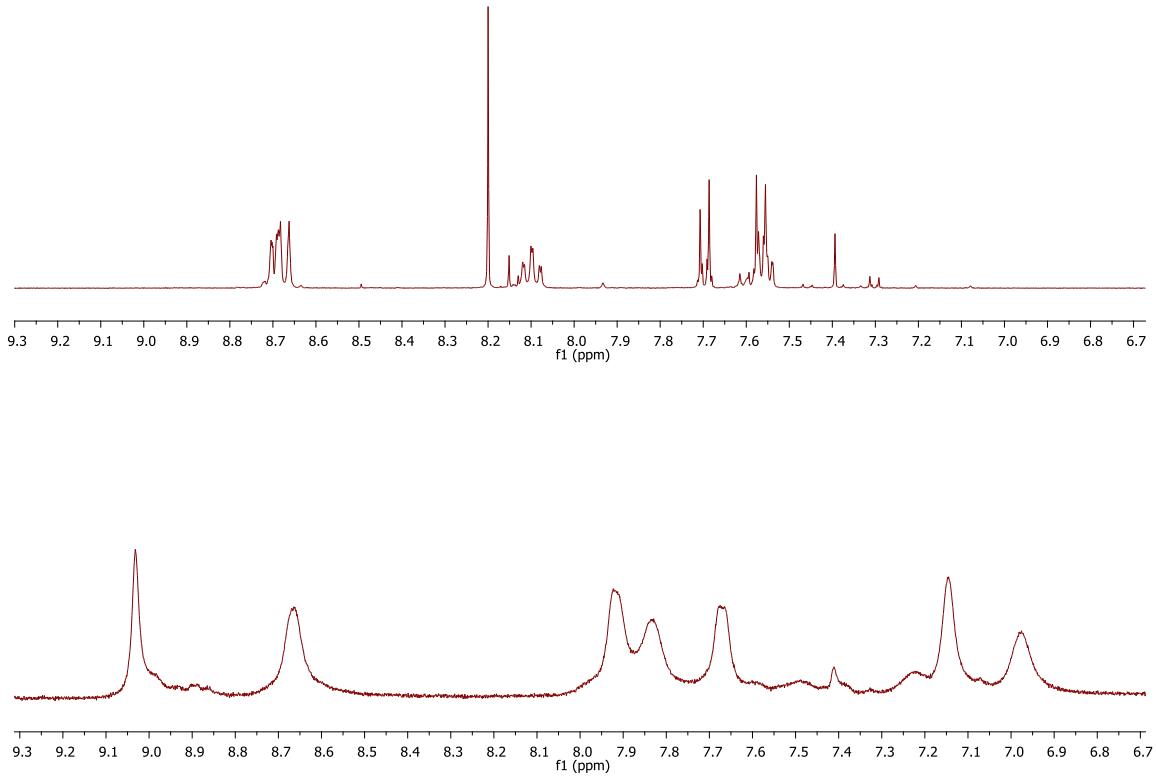

Figure 18 – Stacked ^{1}H NMR plot including monomer (top) and iron coordination polymer (bottom).

The other significant change between the monomer and polymer spectra is the change in chemical shift of all of the signals. The five hydrogen atoms on the terpyridine moiety are all part of the aromatic system coordinating to the metal centre and as such it is reasonable that they experience a change in electronic environment and therefore chemical shift. However, the two unique hydrogen atoms on the thiobisbenzenethiol are 6 and 7 bonds removed from the central nitrogen atom coordinating to the metal centre, and 3 and 4 bonds from the aromatic terpyridine moiety, respectively. Being so far removed from the metal centre one would expect that the electronic environment of these hydrogen atoms would not change enough to result in a significant shift in signal, and had

these aromatic hydrogens been attached to terpyridine with ether instead of thioether linkages, one would likely be correct. The fact that these two hydrogens experience a chemical shift suggests that the conjugation extends throughout the entire organic monomer which is allowed due to the thioether linkages.

2.4.2 – Viscometric Analysis

As the synthesized polymer was not a viable candidate for GPC analysis due to both its limited solubility and the presence of cationic iron, viscometry was utilized in order to obtain a rough estimate of the chain length of the coordination polymer.[78,89,90] The Ostwald viscometer was first calibrated with a solvent of known viscosity, DMF. Next, a qualitative measurement was performed by determining the relative viscosity for concentrated solutions of the coordination polymer, the uncoordinated monomer, and a polymer of known molecular weight. The times required for a precise volume of each solution, with equivalent mass concentration, to flow through the viscometer as well as their calculated relative viscosities (η_{rel}) are collected in Table 1. Polyethylene glycol 1000 was chosen as the polymer of known molecular weight, and while it is certainly not an ideal model for the coordination polymer, its main purpose is to be used as a reference for the quantitative measurements.

Table 1 – Flow time and relative viscosities for measured solutions.

Compound	Flow Time (s)	Relative Viscosity
DMF (pure solvent)	87	1
Monomer	95	1.09
Iron Coordination Polymer	179	2.06
PEG 1000	128	1.47

Relative viscosity is so named because the values are relative to that of the pure solvent being used.[78] As such, pure DMF has a relative viscosity of 1 and the three solutions have viscosities larger than that value. While these values are simply an initial qualitative investigation, it is interesting to note that with solutions of nearly identical mass concentration the coordination polymer has a relative viscosity nearly double that of the monomer, and significantly larger than PEG 1000.

The more useful data derived from viscometry is a quantitative, albeit approximate, determination of the polymer molecular weight. In order to determine this value, the intrinsic viscosity ($[\eta]$) must first be determined.[91] It is important to note that measurements performed with the intent to determine intrinsic viscosity must be performed at relatively low concentrations. The flow times of a dilution series are used to determine the relative viscosities of each solution, and the calibration constant of the viscometer is further used to determine the specific viscosity (η_{sp}) for each. The values

of $\frac{\ln(\eta_{rel})}{c}$ and $\frac{\eta_{sp}}{c}$ are determined, as can be seen in Table 2, and are then plotted as functions of the concentration. These plots can be seen in Figures 19 and 20. The intrinsic viscosity is then determined by extrapolating to the y-intercept, or the point where the concentration is zero.

Table 2 – Plotted values to determine intrinsic viscosities.

Concentration (mg/mL)	$\boldsymbol{\frac{\ln(\eta_{rel})}{c}}$	$\boldsymbol{\frac{\eta_{sp}}{c}}$
Iron Coordination Polymer		
4	11.19	11.75
8	10.65	12.13
12	10.46	12.27
PEG 1000		
4	5.67	6.103
8	5.593	6.232
12	5.421	6.486

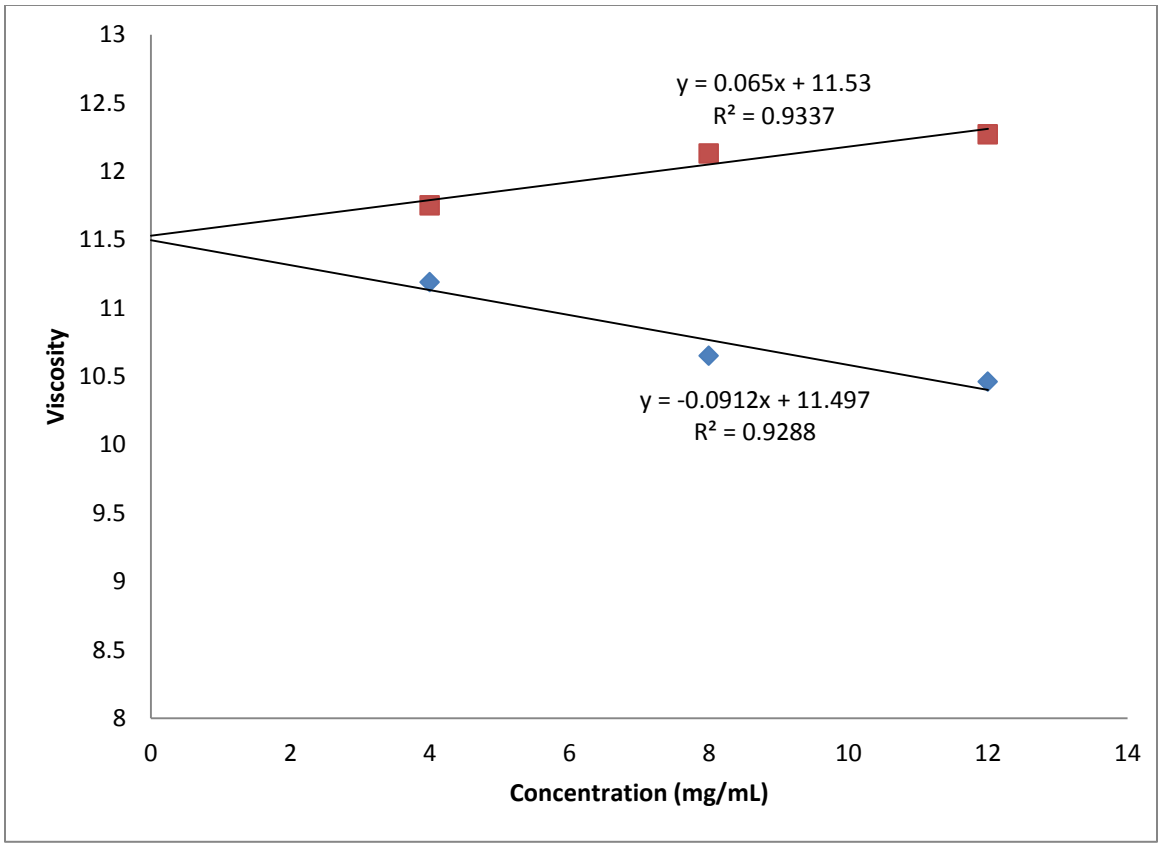

Figure 19 – Viscosity plots of η_{sp}/c (top) and $\ln(\eta_{rel})/c$ (bottom) to determine the intrinsic viscosity of the iron coordination polymer.

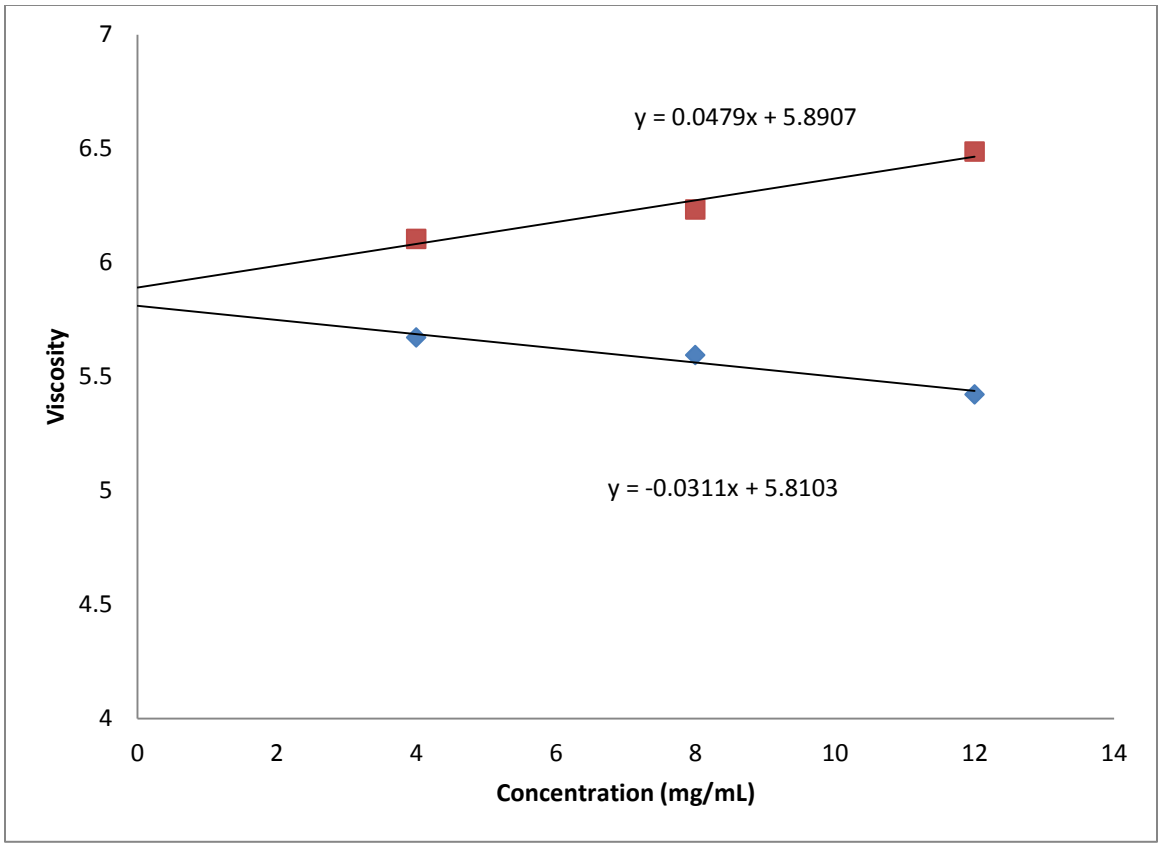

Figure 20 – Viscosity plots of η_{sp}/c (top) and $\ln(\eta_{rel})/c$ (bottom) to determine the intrinsic viscosity of PEG 1000.

The two different viscosity plots in both Figures 19 and 20 are theoretically redundant as the intercept for each series should be identical. Both are traditionally plotted as a means to check the precision of the experimental results, and as the results differ slightly the average of the two intercepts was used as the intrinsic viscosity of each polymer which can be seen in Table 3. The intrinsic viscosity is related to the molecular weight of a polymer through the Mark-Houwink Relationship:[78]

$$[\eta] = KM^a \quad \textbf{(1)}$$

which can be rearranged to:

$$M = \left(\frac{[\eta]}{K}\right)^{\frac{1}{a}} \quad \textbf{(2)}$$

where [η] is the intrinsic viscosity, *M* is the molecular weight of the polymer, *K* is the Mark-Houwink parameter related to the polymer-solvent system, and *a* is the Mark-Houwink parameter that relates to the flexibility and shape of the polymer chain.[92]

It is at this step where the calculation truly turns into an approximation, as *K* and *a* can only be obtained experimentally and therefore must be estimated for a polymer of unknown molecular weight. It is also the step where the purpose of the PEG measurement becomes apparent, as it is a known polymer used to give insight into the precision of the procedure. As the two Mark-Houwink parameters can only be obtained experimentally, if they have not already been determined for the specific polymer (which is impossible for a novel polymer with an unknown molecular weight) and the specific polymer-solvent system, *K* and *a* cannot be known. Instead they must be approximated using known parameter values from similar polymers and polymer-solvent systems.[93] Using these approximated values and equation 2, the molecular weights of the iron coordination polymer and PEG 1000 were calculated and can be seen in Table 3.

Table 3 – Calculated intrinsic viscosities and molecular weights.

Polymer	**Intrinsic Viscosity [η]**	**Molecular Weight (g/mol)**
Iron coordination polymer	11.514	38320
PEG 1000	5.851	858.8

As can be seen in Table 3, the molecular weight of PEG 1000 was determined to be 858.8 g/mol, which is an underestimation, but within 15% of the correct value. Using the same method, the iron coordination polymer was determined to have a molecular weight of nearly 40,000 g/mol. Using this value and the molecular weight of 1058.68 g/mol for the monomeric unit, it can be estimated that the polymer chains are comprised of, on average, 36 subunits.

2.4.3 – Thermal Analysis of Polymer

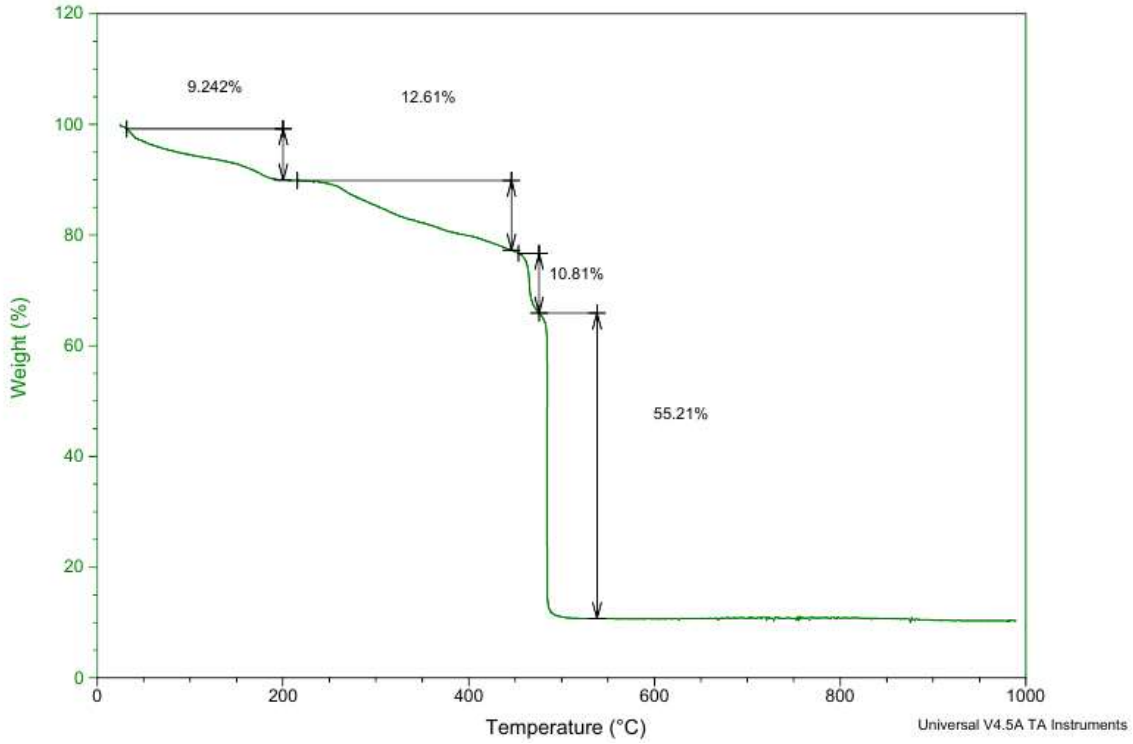

Figure 21 – Thermogram of iron polymer in air.

The thermogram of the iron coordination polymer (Figure 21) was obtained using high resolution TGA under an air atmosphere. High resolution TGA is obtained by heating the sample at a much higher rate than conventional TGA, but the rate is not constant. In high resolution TGA, the heating rate is quite high, as much as 50°C per minute, but when a mass loss is detected the heating rate is decreased until the mass loss event ends. As a result, high resolution TGA can be performed quicker, and as the name implies, yields a higher resolution thermogram than conventional TGA.

The iron coordination polymer experiences four decompositions, with the final one occurring just below 500°C. The first decomposition up to 200°C is a result of the

loss of moisture adsorbed onto the polymer as well the loss of any residual solvent. The second gradual decomposition, from 200°C to 450°, and the third decomposition, at 450°C, are a result of the loss of the first and then second hexafluorophosphate counterions. This occurs in two steps due to the increased attraction of the second, lone anion to the cationic iron centre. Assuming that the first decomposition is the loss of solvent and moisture, the second and third decompositions account for a loss of 25.8% of the mass of the actual polymer, which agrees well with the fact that the hexafluorophosphate anions account for 27.4% of the mass of each monomeric unit of the polymer.

The final mass loss is a result of the decomposition of organic bis-terpyridine monomeric unit of the polymer. This organic monomer accounts for 67.3% of the mass of the polymer, and agrees reasonably well with this loss, which is 61.0% of the polymer mass loss when correcting for the first decomposition. The remaining mass is likely caused by the presence of non-volatile iron oxides, which agrees with the percentage of the polymer's mass that is due to the coordinated iron atoms.

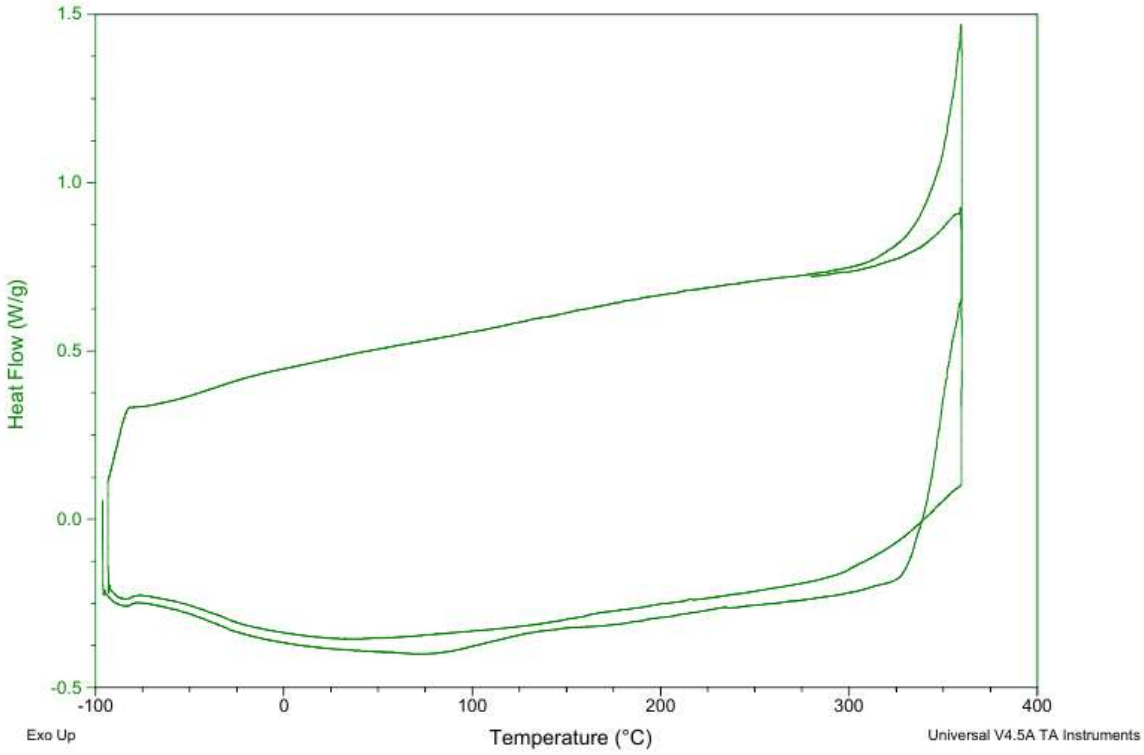

Figure 22 – Differential scanning calorimetry plot of iron coordination polymer, full heat-cool-heat cycle.

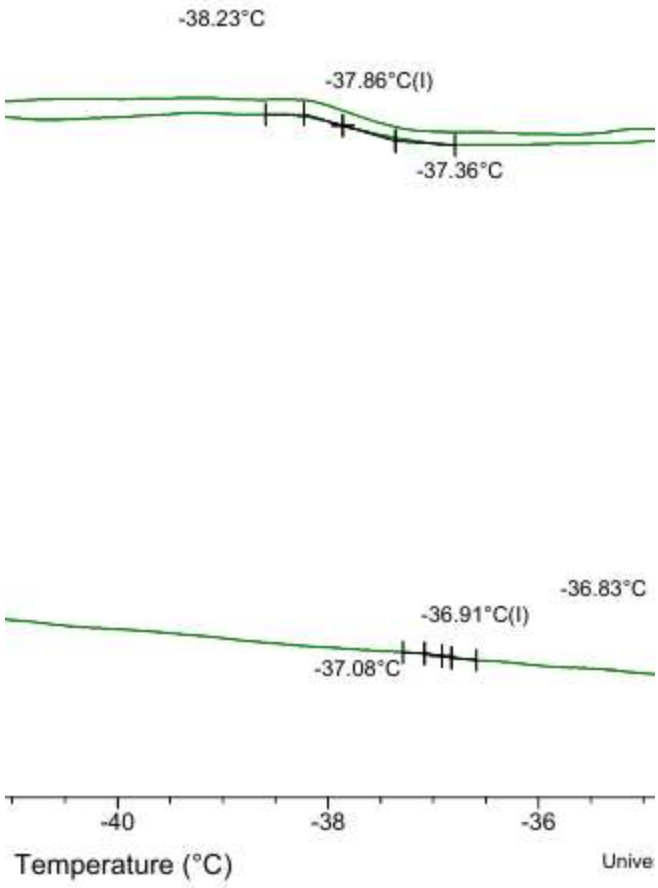

Figure 23 – Differential scanning calorimetry plot of iron coordination polymer highlighting the glass transition point. Top two curves represent heating cycle, bottom curve represents cooling cycle.

Differential scanning calorimetry is used to identify thermal events in the sample material, and as such is often carried out in a heat-cool-heat cycle, as can be seen in Figure 22. This doubling of the heating cycle is performed in order to confirm reversibility of any detected thermal events.

It is practically impossible to identify the glass transition point in the full DSC plot, Figure 22, but when focused on the area of interest, the event is visible. In order to

obtain a better defined DSC plot featuring the glass transition point, a heat-cool-heat experiment was run centred on this point from -46 °C to -34 °C with a reduced heating and cooling rate, as shown in Figure 23. As a result, the glass transition point of the iron coordination polymer was determined to be -37.86 °C. Below this temperature the polymer exists as a brittle, glass-like material, and above the temperature it is amorphous.

2.4.4 – Conductivity Analysis of Polymer

The iron coordination polymer is made up of terpyridine-iron coordination complexes as well as a backbone containing alternating sulphur and phenyl groups. Organometallic terpyridine complexes are known to exhibit charge transfer behaviour,[94,95] and the thioether linked phenyl groups in the backbone provided an extended conjugation system. As such, it was expected that the iron coordination polymer would exhibit conductivity. Further support for this hypothesis is provided in the ^{1}H NMR spectrum of the polymer, as even signals distant to the coordination site are affected by the coordination of iron, implying that there is a long range change to the electronic environment resulting from extended conjugation. Unfortunately, the coordination polymer did not display conductive properties.

It is however possible that the polymer *could* become conductive if an appropriate method of doping were discovered. The iron coordination centre, and therefore the stability of the polymer, is sensitive to oxidation and reduction. As a result, the doping process was limited to more gentle doping methods, which may have been insufficient to narrow the band gap appropriately. The first method of doping attempted was the doping

of the polymer in the solution phase with low concentrations of iron(III) chloride. The second method involved exposing the polymer in the solid phase to iodine vapours.[96] This method was carried out in an iodine chamber, with solid iodine allowed to sublime to the gas phase.[97] The polymer was exposed to this iodine vapour both as a pressed pellet in an attempt to surface dope the bulk material and as a powder that was later turned into a pressed pellet with a hydraulic press.

Conductivity measurements of the polymer using a pressed pellet were performed using both the Van der Pauw method and the co-linear four point probe method. Both techniques showed no conductivity for the polymer, implying that the polymer is either nonconductive or conductive to a magnitude lower than the detection limit of the instruments used.

As mentioned, the polymer could still be potentially conductive under appropriate doping conditions. Future work should be done to determine a gentle, yet effective technique to dope the polymer. Conversely, it is possible that the monomer could be oxidized or reduced using more aggressive techniques prior to polymerization, resulting in an already doped polymer.

2.4.5 – Other Characterization Techniques

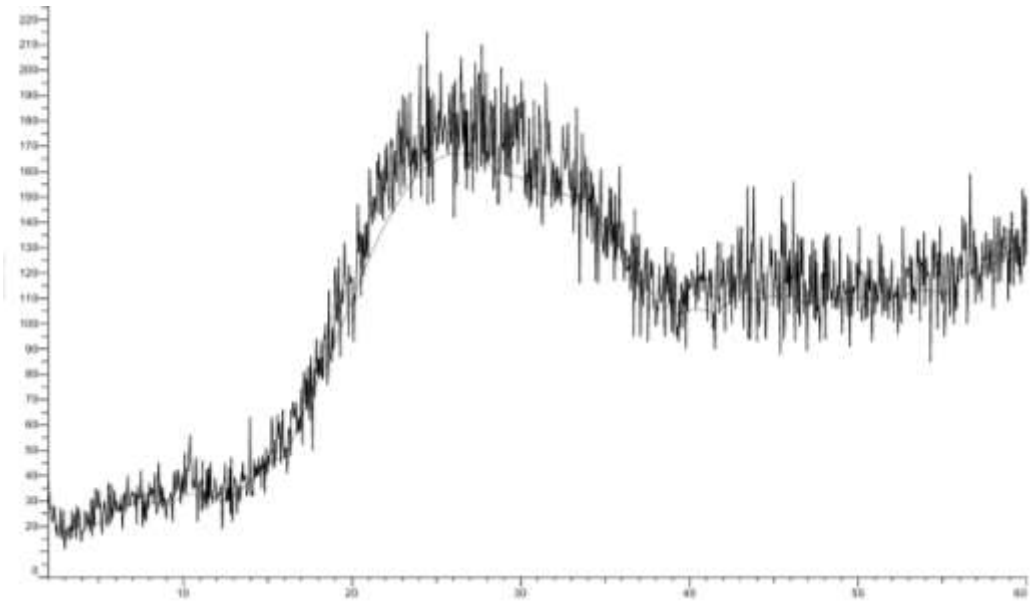

Figure 24 – Diffractogram of iron coordination polymer.

One of the most important properties powder XRD can determine is the crystallinity of a sample, and in cases where it can be compared to library data, this can be used to identify compounds. If a compound is only partially crystalline, powder XRD can help to determine the extent of the compound's crystallinity. In the case of the iron coordination polymer this extent is minimal. This is not a problem, and in fact is similar to the nature of many types of polymers. It is simply the case that the coordination polymer exists as an amorphous compound. This can be determined from the diffractogram of the coordination polymer, as can be seen in Figure 24. Crystalline materials display sharp, highly intense signals in a diffractogram, while amorphous materials lack these signals, and only display a broad, shallow signal. As can be seen in

Figure 24, the coordination polymer matches with the second description, and it can be concluded that it is an amorphous material.

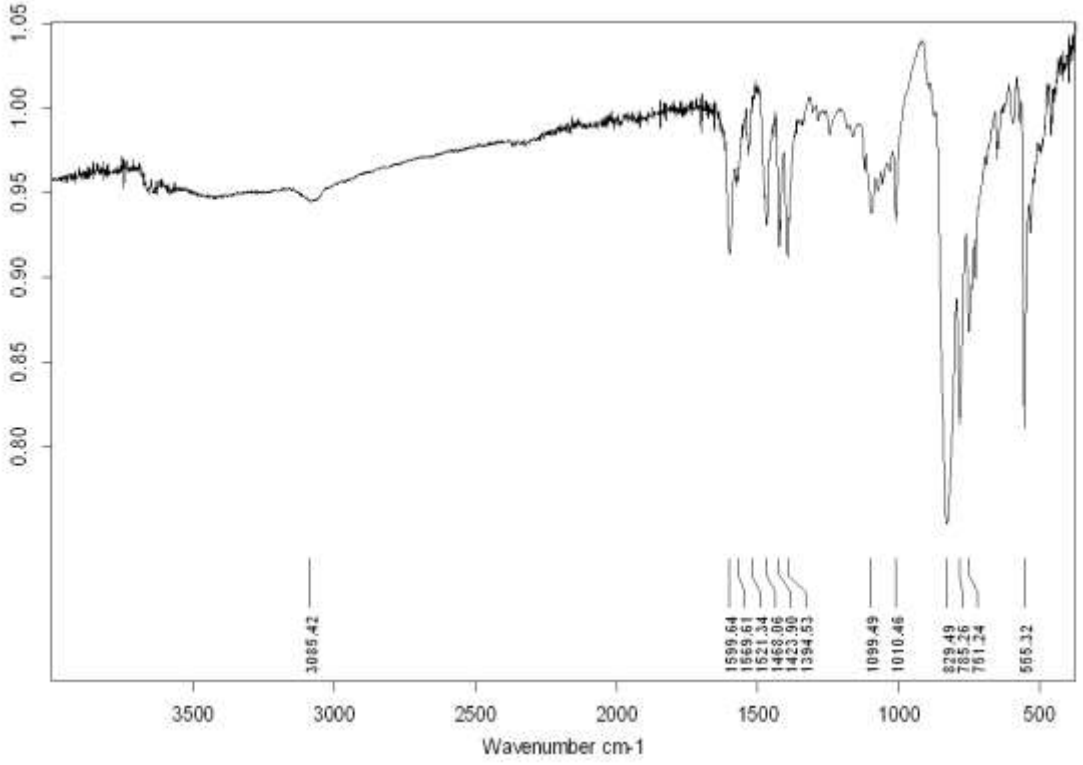

Figure 25 – IR spectrum of iron coordination polymer.

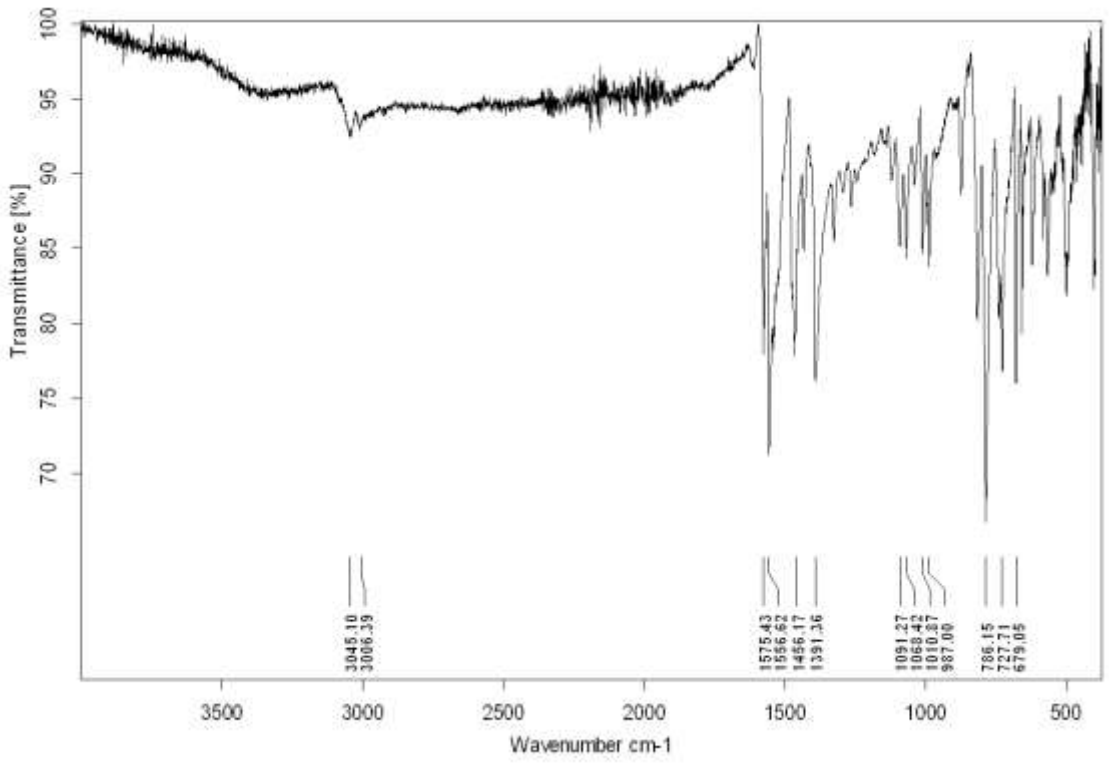

Figure 26 – IR spectrum of bis-terpyridine monomer.

The IR spectrum of the iron coordination polymer (Figure 25) displays a large amount of detail about its structure. Aromatic C-H stretches caused by both the terpyridine and phenyl hydrogens can be seen at 3085 cm^{-1}. The signals between 1599 $cm^{-}1$ and 1394 cm^{-1} correspond to the stretching of the aromatic carbon-carbon and carbon-nitrogen bonds in the pyridyl and phenyl groups of the monomer subunit of the polymer. When compared to the IR spectrum of the monomer, which can be seen in Figure 26, the signals have shifted to higher energies, which is what occurs in iron(II) pyridine coordination complexes.[98] The medium intensity bands at 1099 and 1010 cm^{-1} in Figure 25 correspond to the characteristic 1,4-disubstitution pattern of mononuclear aromatics, and are caused by the phenyl rings in the centre of the organic moiety. The

strong intensity bands present at 829 and 785 cm^{-1} in the spectrum of the iron coordination polymer are a result of the stretching of the fluorine-phosphorous bonds in the hexafluorophosphate counterion of the coordination polymer,[99] and are not present in the spectrum of the monomer.

3 – Synthesis and Characterization of Polymer Series

3.1 – Synthesis of Polymer Series

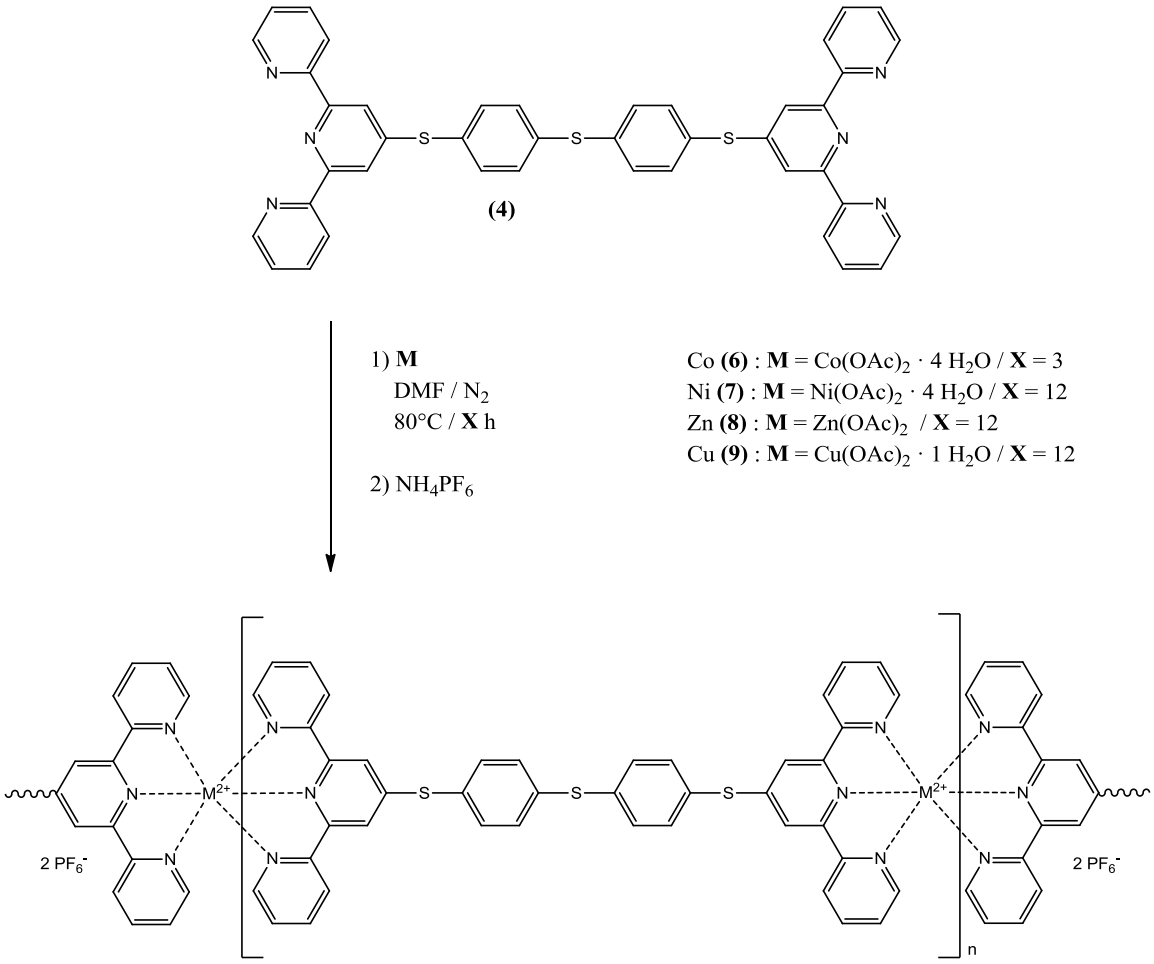

Figure 27 – Synthesis of polymer series.

The polymer series is prepared by a reaction similar to that of the iron polymer, with the exception of the ruthenium polymer, and is modified from literature procedures[100] as can be seen in Figure 27. One equivalent of the bis-terpyridine-substituted monomer is reacted with one equivalent of the appropriate metal acetate and

stirred at 80°C under a nitrogen atmosphere. The coordination reaction does not occur as readily with other transition metals as it does with iron, and it is for this reason that the reactions are heated and some occur over a longer period of time. As with the iron polymer, ammonium hexafluorophosphate is then added to replace the Cl^- counter ions with PF_6^- anions. The solutions are then precipitated dropwise into diethyl ether and collected via vacuum filtration.

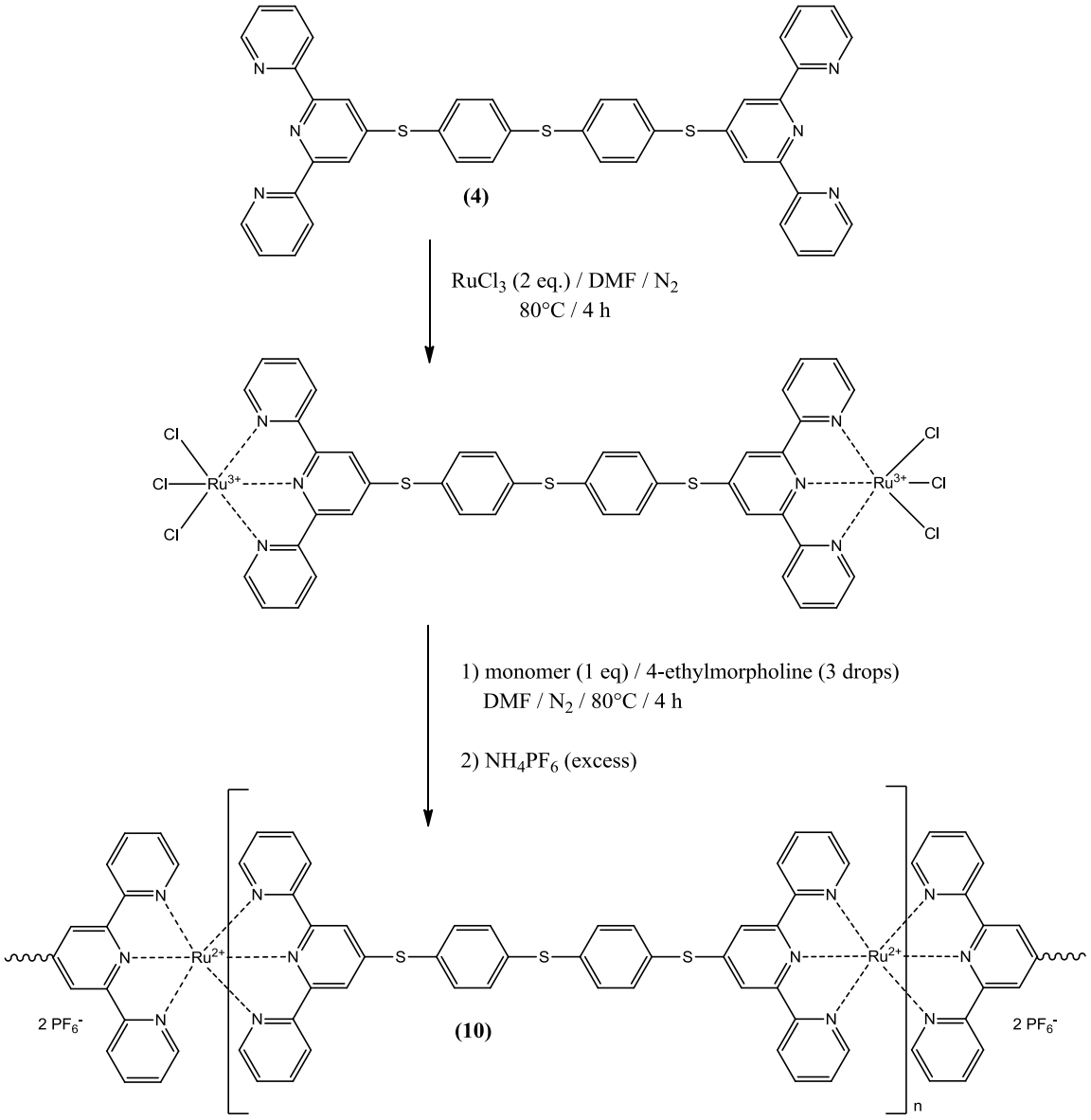

Figure 28 – Synthesis of the ruthenium polymer.

Preparation of the ruthenium polymer deviates even further from that of the iron polymer and is modified from literature procedures[101] as can be seen in Figure 28. One equivalent of the bis-terpyridine-substituted monomer is reacted with two equivalents of $RuCl_3$ at 80°C for 4 hours under a nitrogen atmosphere to afford a stable trichloro

ruthenium coordination complex that does not readily undergo coordination of a second terpyridine ligand. A second equivalent of the monomer is then added along with three drops of 4-ethylmorpholine to reduce the ruthenium, followed by the coordination of the second terpyridine ligand. The reaction solution is stirred for an additional 4 hours at 80°C under a nitrogen atmosphere and the resulting red solution is treated with ammonium hexafluorophosphate and the product collected by precipitation and filtration.

3.2 – Characterization of Polymer Series

3.2.1 – NMR Analysis of Polymer Series

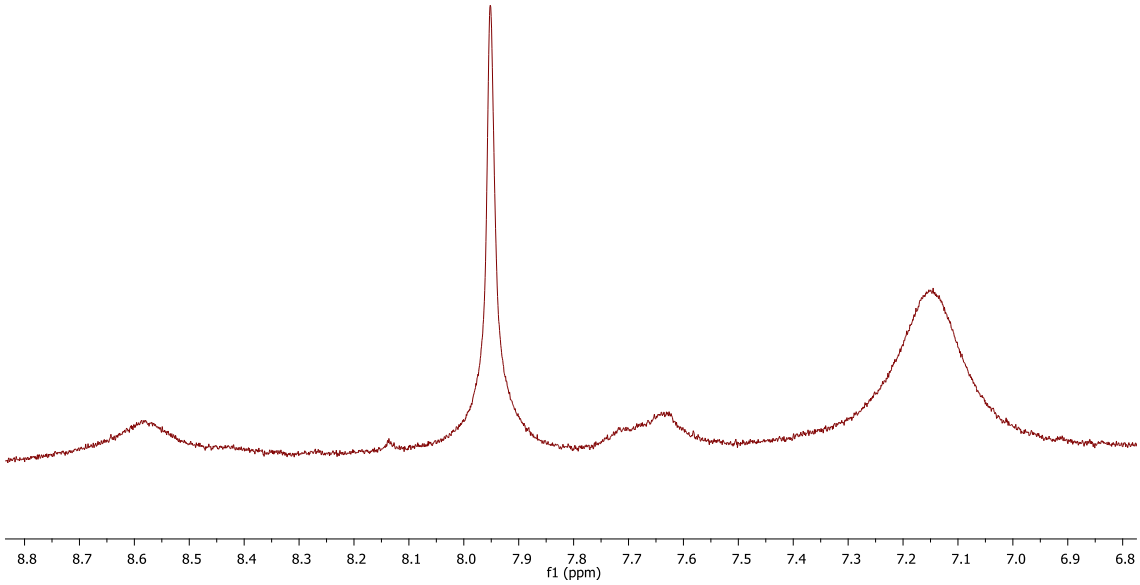

Figure 29 – ^{1}H NMR spectrum of nickel coordination polymer.

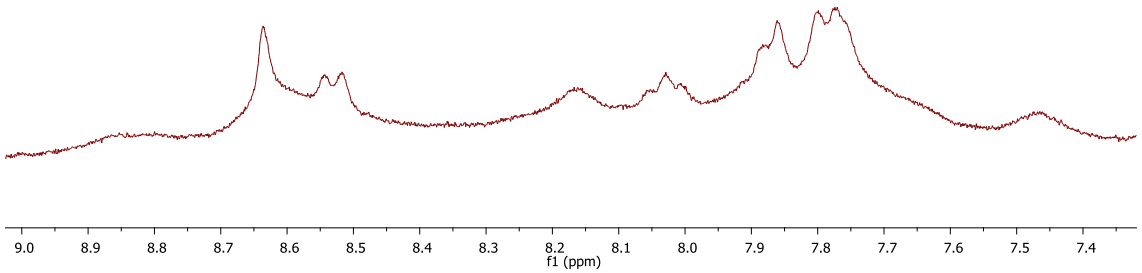

Figure 30 – ^{1}H NMR spectrum of zinc coordination polymer.

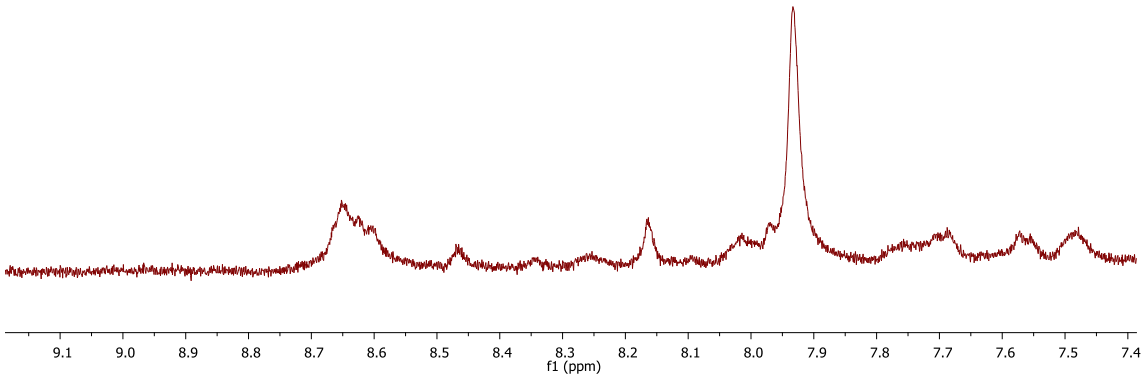

Figure 31 – ^{1}H NMR spectrum of ruthenium coordination polymer.

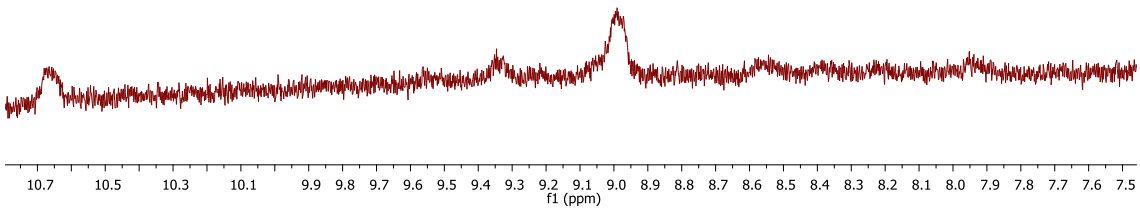

Figure 32 – ^{1}H NMR spectrum of cobalt coordination polymer

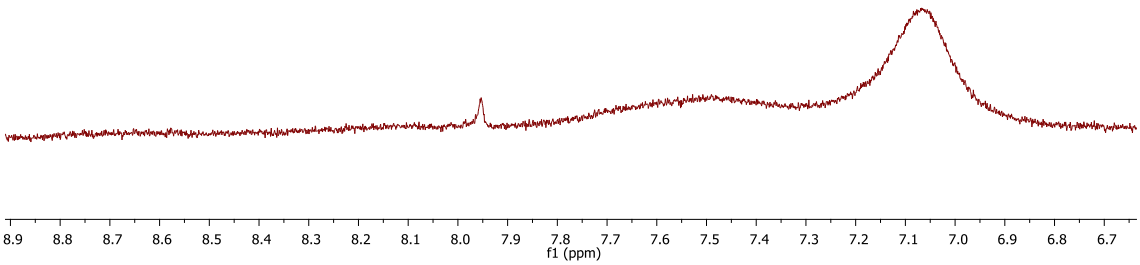

Figure 33 – ^{1}H NMR spectrum of copper coordination polymer.

The proton NMR spectra of the compounds in the coordination polymer series were obtained and can be seen in Figures 29 through 33. While the spectra for the nickel, zinc, and ruthenium polymers show the expected signal broadening caused by polymerization, the spectra for the copper and cobalt polymers contain very few signals. This was, however, also expected and is a result of the paramagnetic nature of these two compounds. The cobalt centre exists as a Co^{2+} species with seven d-electrons, and the copper centre exists as a Cu^{2+} species with nine d-electrons. As a result, both possess an unpaired electron, resulting in their paramagnetic nature. Paramagnetic compounds have characteristically wide chemical shift ranges and experience signal broadening. As a result, the appearance of the spectra in Figures 32 and 33 are not unexpected.

3.2.2 – Fluorescence Analysis

Terpyridine is known to exhibit fluorescent behaviour, and as such several sample compounds from the polymer series were analysed via fluorimetry in a solution of DMF. The monomer, which contains two terpyridine groups joined with a conjugated organic linker was expected to exhibit a relatively high degree of fluorescence, while most of the polymers would display reduced fluorescence. This is due to the fact that the polymers are formed by the conjugation of terpyridine to various cationic transition metals which results in quenching of the fluorescence. The zinc containing polymer was expected to be an exception to this as the Zn^{2+} coordination centre is a d^{10} system and should therefore not cause any, or at least a very small degree of, fluorescent quenching. As a result, the zinc containing polymer was expected to display a degree of fluorescence similar to that of the monomer. As can be seen in Figure 34, this was not the case.

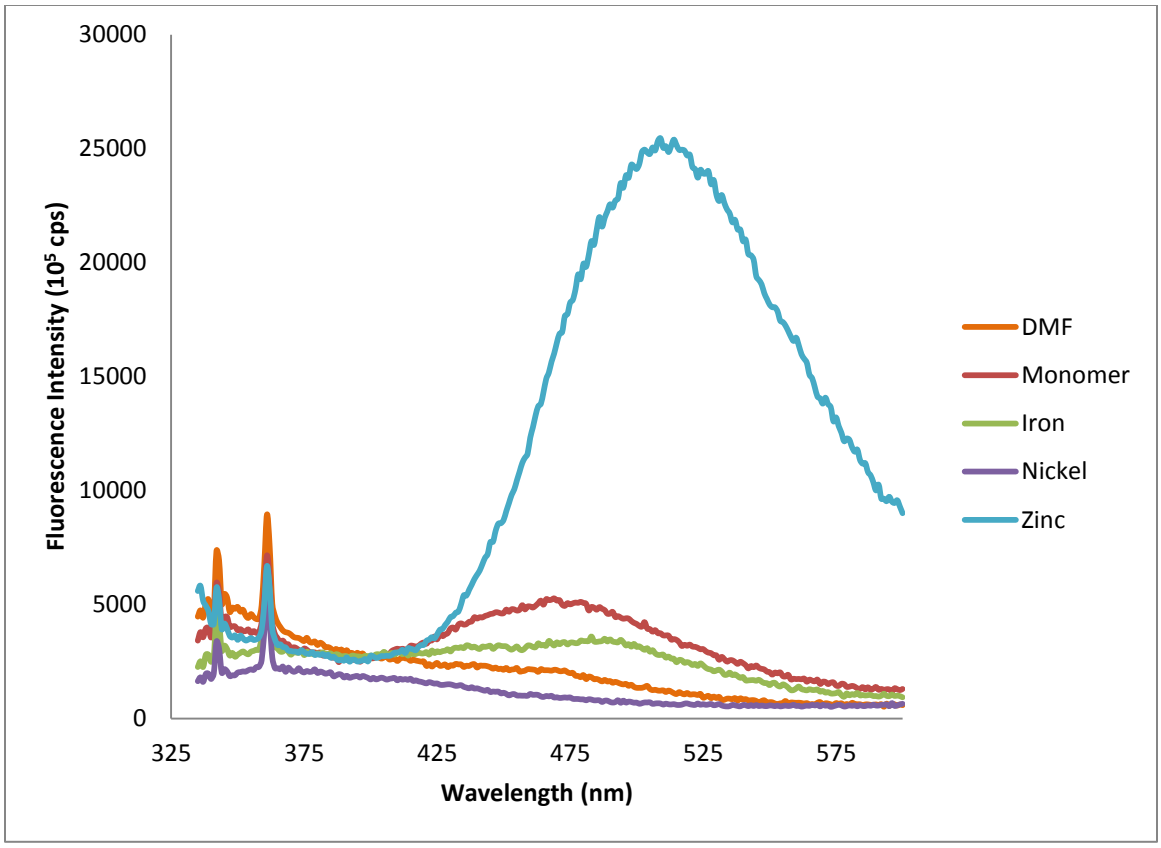

Figure 34 – Fluorescence plots of several sample polymers solutions with similar absorbances.

As anticipated, the monomer proved to be fluorescent, although perhaps not to the degree expected when compared to other examples of fluorescent terpyridine compounds.[102,103] The results for the iron and nickel polymer were also as expected, with both displaying a reduced fluorescence as a result of fluorescent quenching. On the other hand, the results for the zinc polymer were both unexpected and exciting. As can be seen in Figure 34, the zinc polymer displayed a large degree of fluorescent enhancement, with its intensity being approximately five times that of the monomer alone.

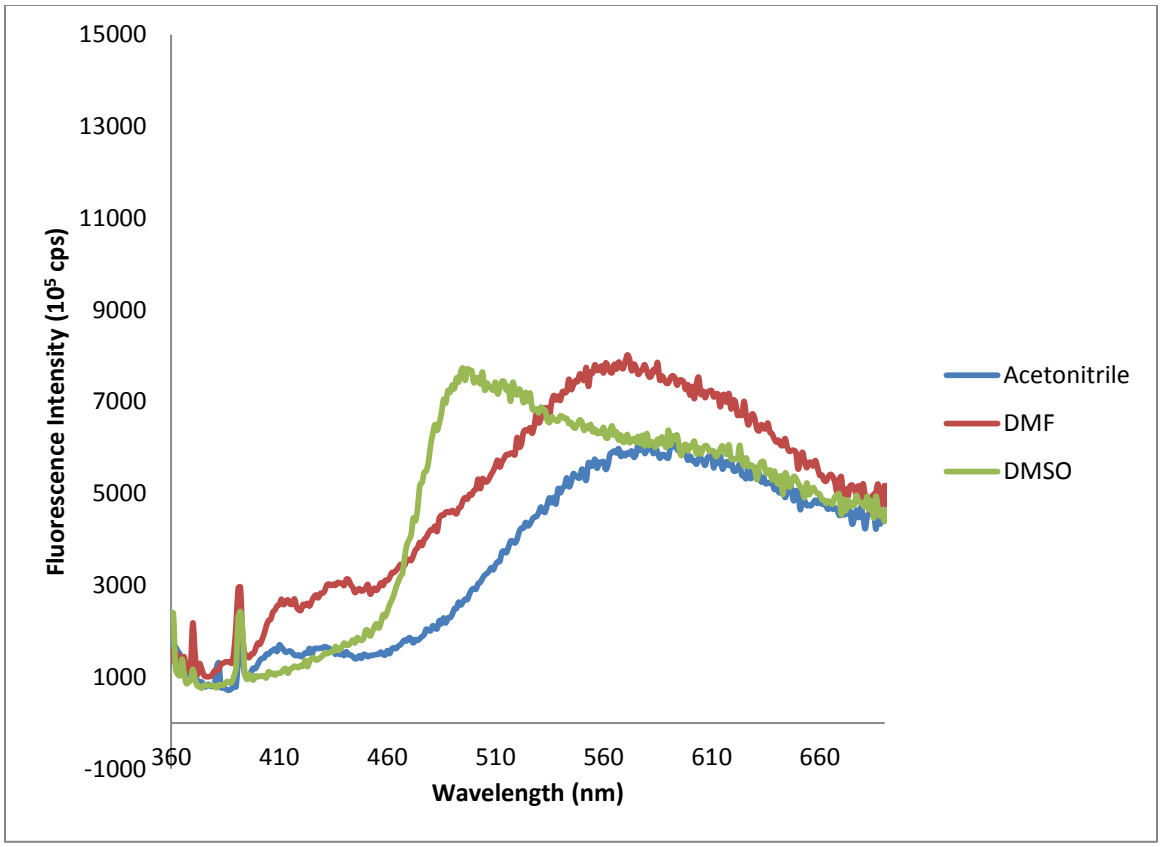

Figure 35 – Solvent effect investigation of zinc polymer.

The effects of different solvents on the zinc coordination polymer were then investigated, and can be seen in Figure 35. The plots for the polymer in DMF and acetonitrile were very similar, while the plot of the polymer in DMSO varied significantly. This is expected, and is a result of the increased polarity of DMSO as compared to DMF and acetonitrile. The dielectric constant of a solvent is a good approximation of the relative polarity of that solvent, and the dielectric constants of the three solvents used are shown in Table 4. As can be seen, DMF and acetonitrile have a very similar dielectric constant, while that of DMSO differs significantly.

Table 4 – Dielectric constants and wavelengths of maximum fluorescence for the three solvents.[104]

Solvent	**Dielectric Constant (ε)**	**λ_{max} (nm)**
Acetonitrile	36.64	578
DMF	38.25	571
DMSO	47.24	495

The observed change in the fluorescence spectrum is a direct result of the effect that a solvent has on the energy gap between the excited and ground electronic state of the molecule. Solvents of increasing polarity cause an increase in this energy gap, and as a result the electronic relaxation will result in the fluorescent release of a higher energy photon. As can be seen in Table 4, DMSO has a larger dielectric constant than the two other solvents and is therefore more polar. As a result, the polymer in DMSO releases a higher energy photon via fluorescence, which can be observed as the blue shift of the fluorescent spectrum in DMSO as seen in Figure 35. The opposite of this is usually the case however, with an increase in solvent polarity resulting in a red shifted spectrum. The fact that this spectrum displays a blue shift implies that the molecule's ground state is more polar than the excited state. Another interesting feature in this plot is the change in shape of the spectrum of the polymer in DMSO, although the cause of this is not clear.

In order for the fluorescent quantum yield for the zinc containing polymer to be determined using equation 3, absorbance and fluorescence measurements were taken for

the polymer in three different solvents as well as a reference standard, 9,10-diphenylanthracene in cyclohexane. These four fluorescence plots can be seen in Figures 36 and 37.

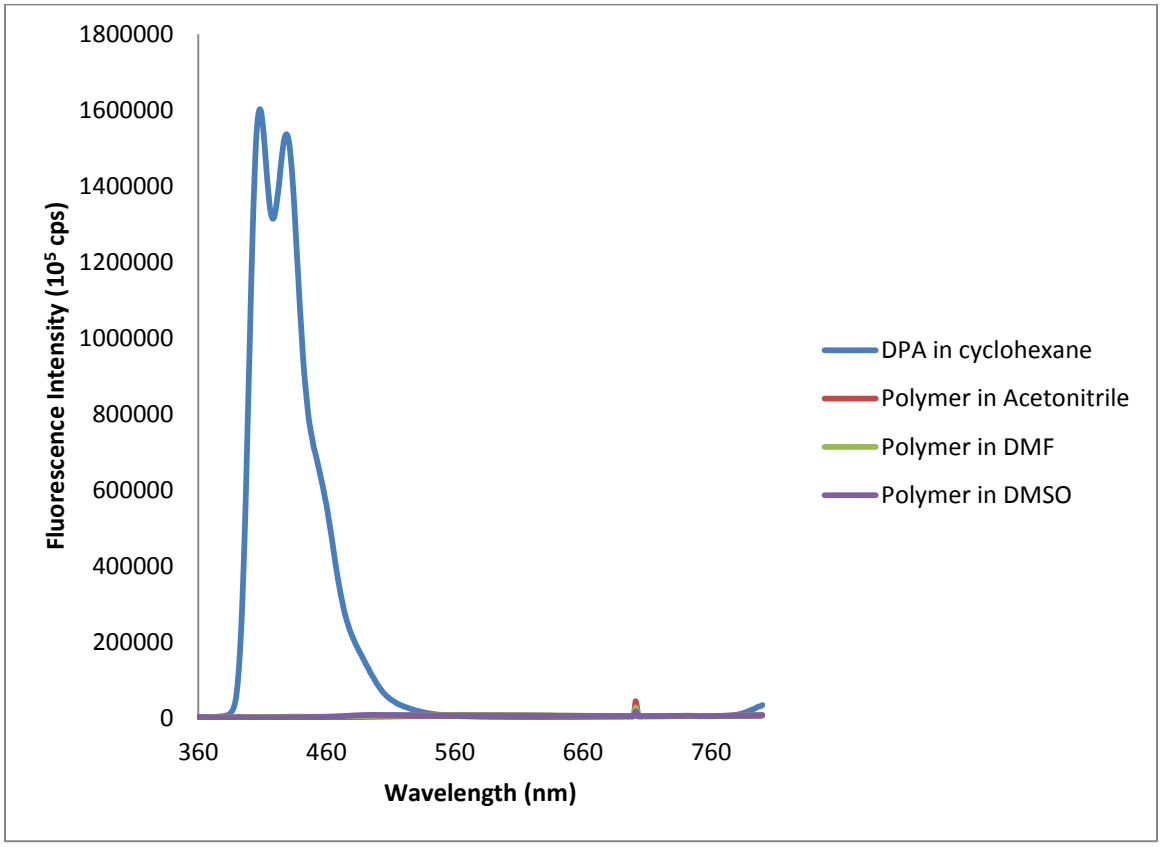

Figure 36 – Fluorescence plots for quantum yield calculations at full intensity.

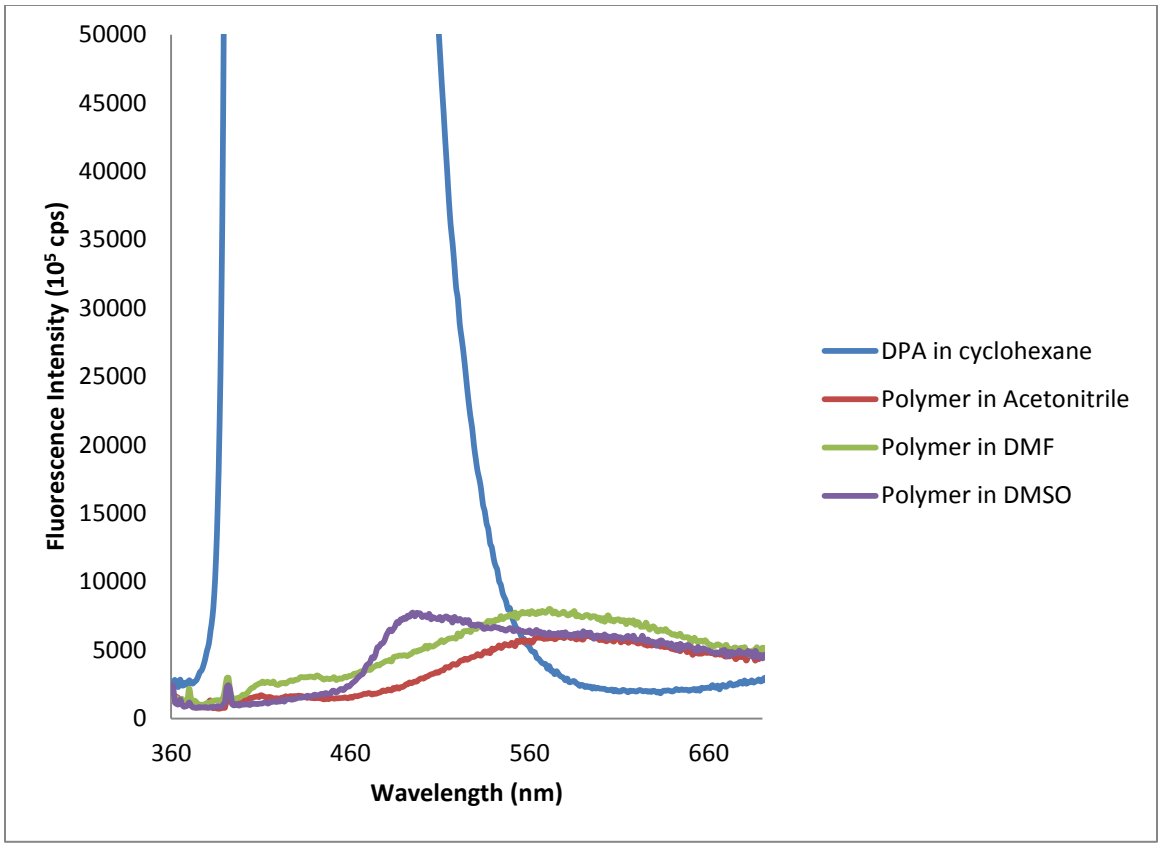

Figure 37 – Fluorescence plots for quantum yield calculations scaled to intensity of polymer.

The absorbance of each system was recorded at the excitation wavelength, 350 nm and the integrated area under the fluorescence curves was also obtained for each system with the removal of a solvent blank similarly applied. These values can be seen in Table 5.

Table 5 – Values for quantum yield calculations.

Solvent	Fluorescence (integrated area)	Absorbance	Refractive Index[105]
Diphenyl Anthracene (standard)			
Cyclohexane	87039314	.098438	1.4235
Zinc Polymer			
Acetonitrile	901617.2	.260389	1.3442
DMF	1091659.2	.376678	1.4305
DMSO	1150096	.430216	1.4793

These values were then applied to equation 3,

$$\boldsymbol{\phi_{F,S}} = \boldsymbol{\phi_{F,R}}\, \boldsymbol{x}\, \left(\frac{\boldsymbol{F_S}}{\boldsymbol{F_R}}\right)\, \boldsymbol{x}\, \left(\frac{\boldsymbol{A_R}}{\boldsymbol{A_S}}\right)\, \boldsymbol{x}\, \left(\frac{\boldsymbol{n_S}}{\boldsymbol{n_R}}\right)^{\boldsymbol{2}} \qquad \textbf{(3)}$$

where $\boldsymbol{\phi_{F,S}}$ is the fluorescent quantum yield of the solution, $\boldsymbol{\phi_{F,R}}$ is the fluorescent quantum yield of the reference, F_S is the fluorescence of the solvent, F_R is the fluorescence of the reference, A_R is the absorbance of the reference, A_S is the absorbance of the solution, n_S is the refractive index of the solution solvent, and n_R is the refractive index of the reference solvent. The fluorescent quantum yield values for the three solvent systems were then obtained and these values are tabulated in table 6. As can be seen, the quantum yields were relatively low, which is not unexpected when comparing the three

polymer plots with that of the reference standard, as can be seen in Figures 36 and 37. The quantum yield of the polymer was nearly identical in the three different solvents, with only a slight variation seen in the acetonitrile system.

Table 6 – Calculated values of quantum yield.

Solvent	**Quantum Yield ($\phi_{F,S}$)**
Acetonitrile	3.5×10^{-3}
DMF	3.3×10^{-3}
DMSO	3.3×10^{-3}

3.2.3 – Electron Paramagnetic Resonance (EPR) Analysis.

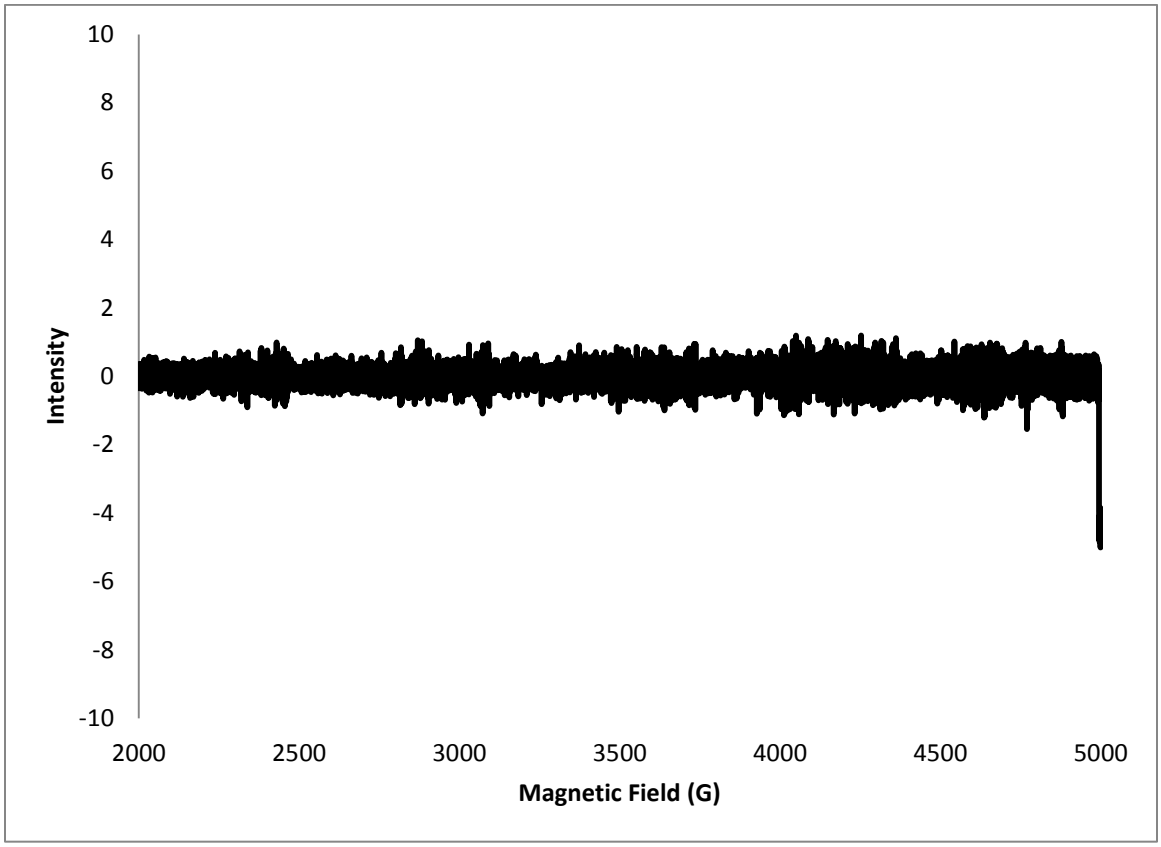

Figure 38 – EPR spectrum of iron coordination polymer obtained at room temperature.

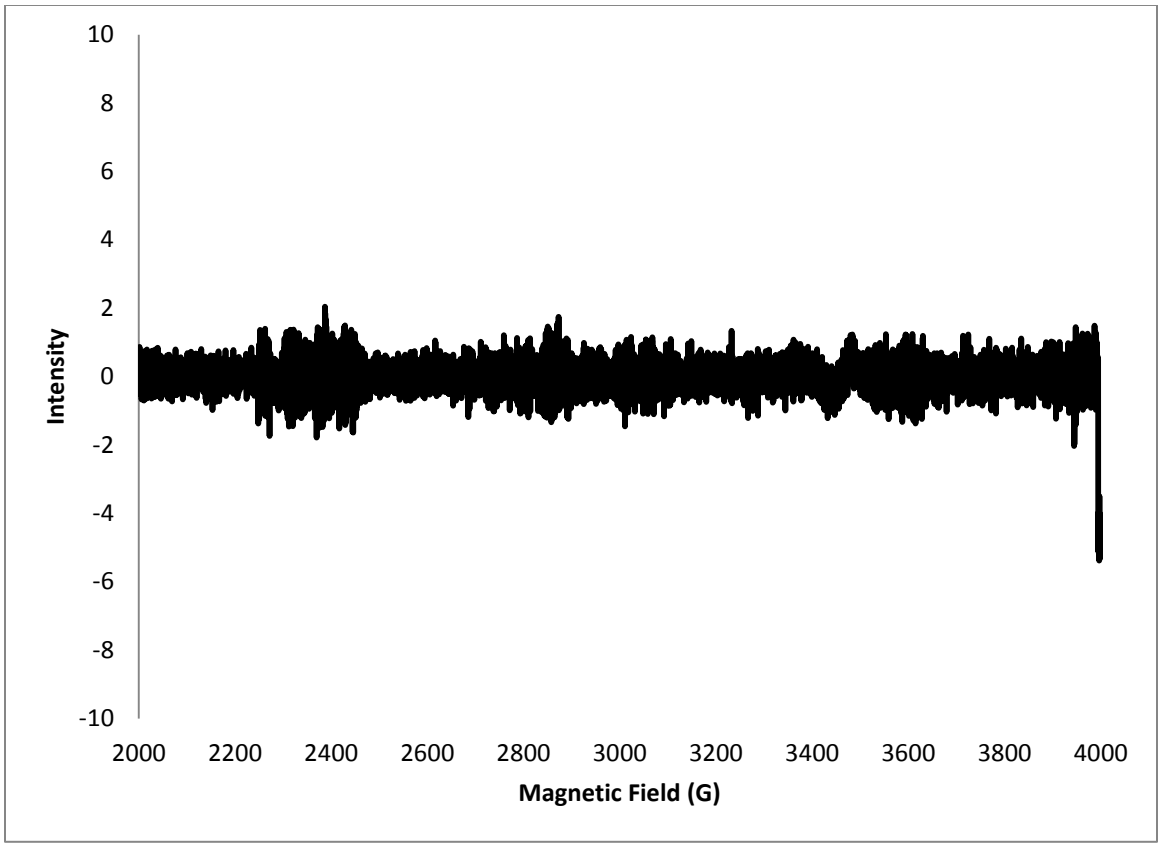

Figure 39 – EPR spectrum of iron coordination polymer obtained at 77 K.

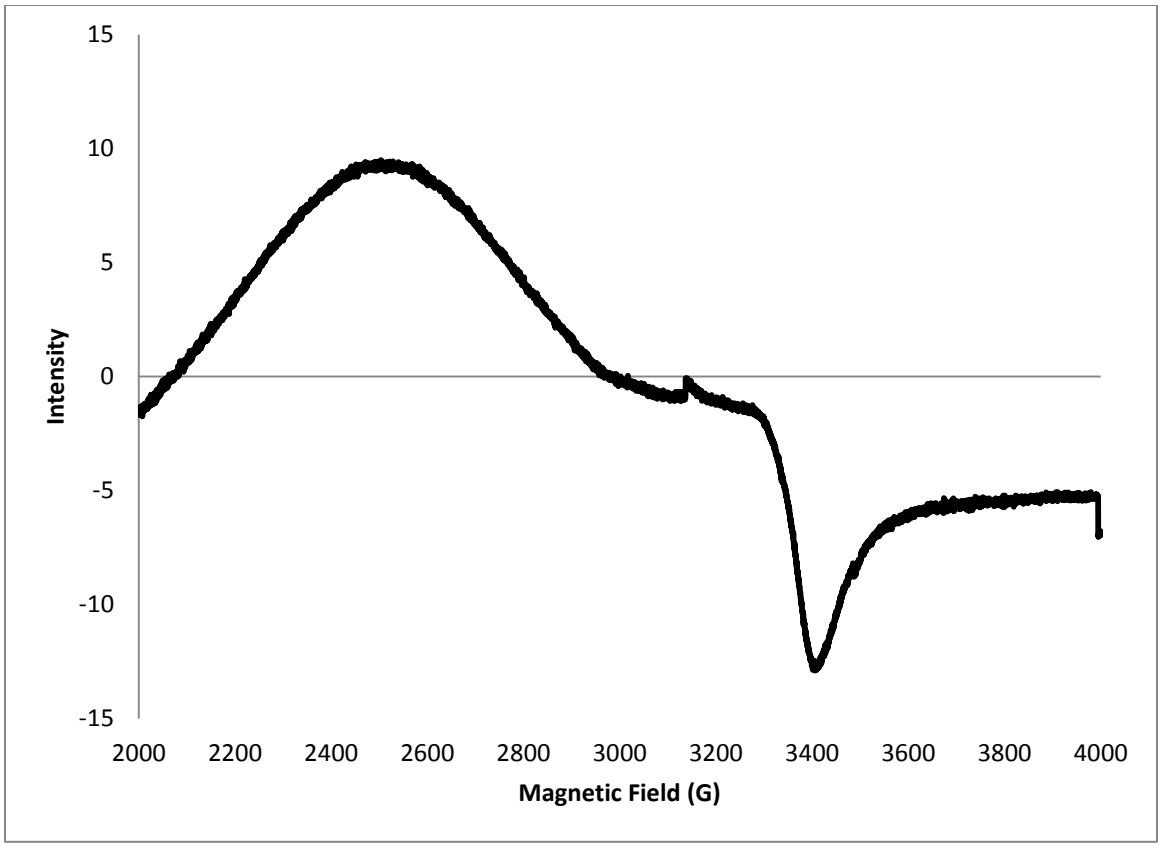

Figure 40 – EPR spectrum of copper coordination polymer obtained at room temperature, multiple scan average.

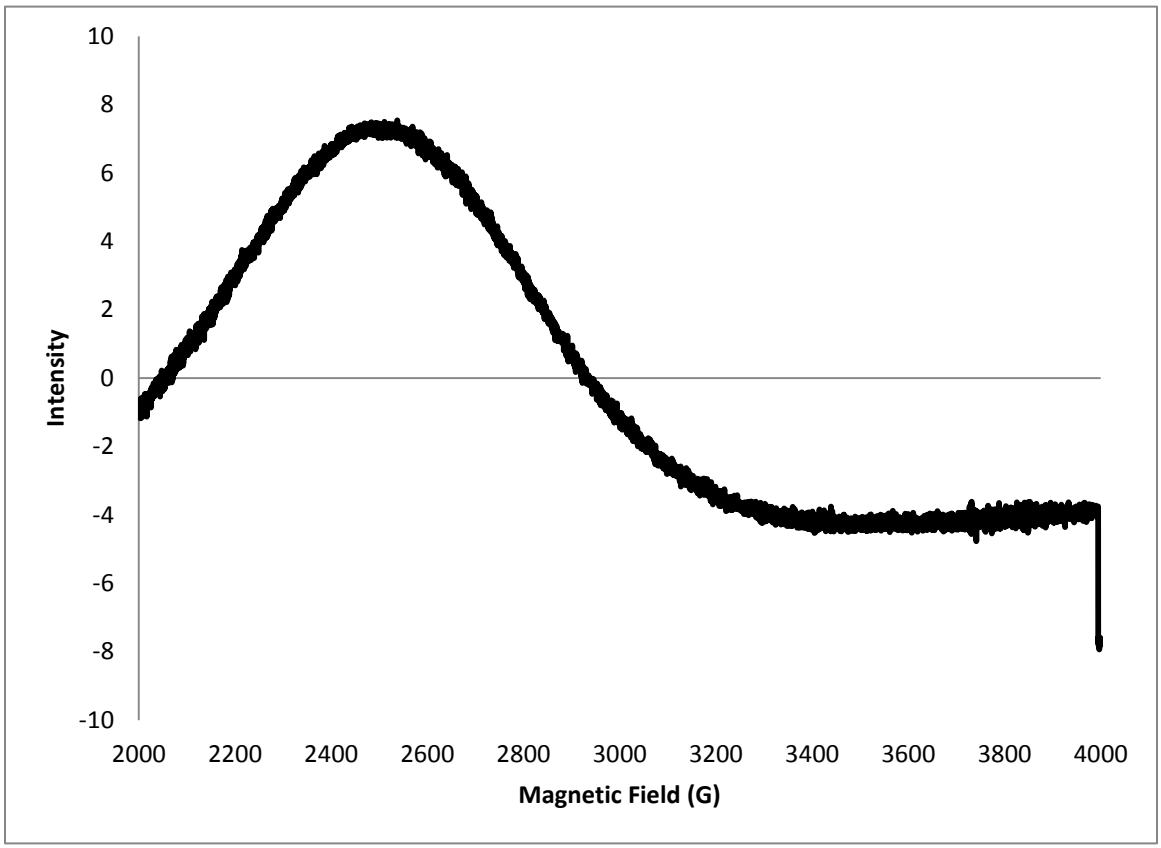

Figure 41 – EPR spectrum of empty quartz tube obtained at room temperature, multiple scan average.

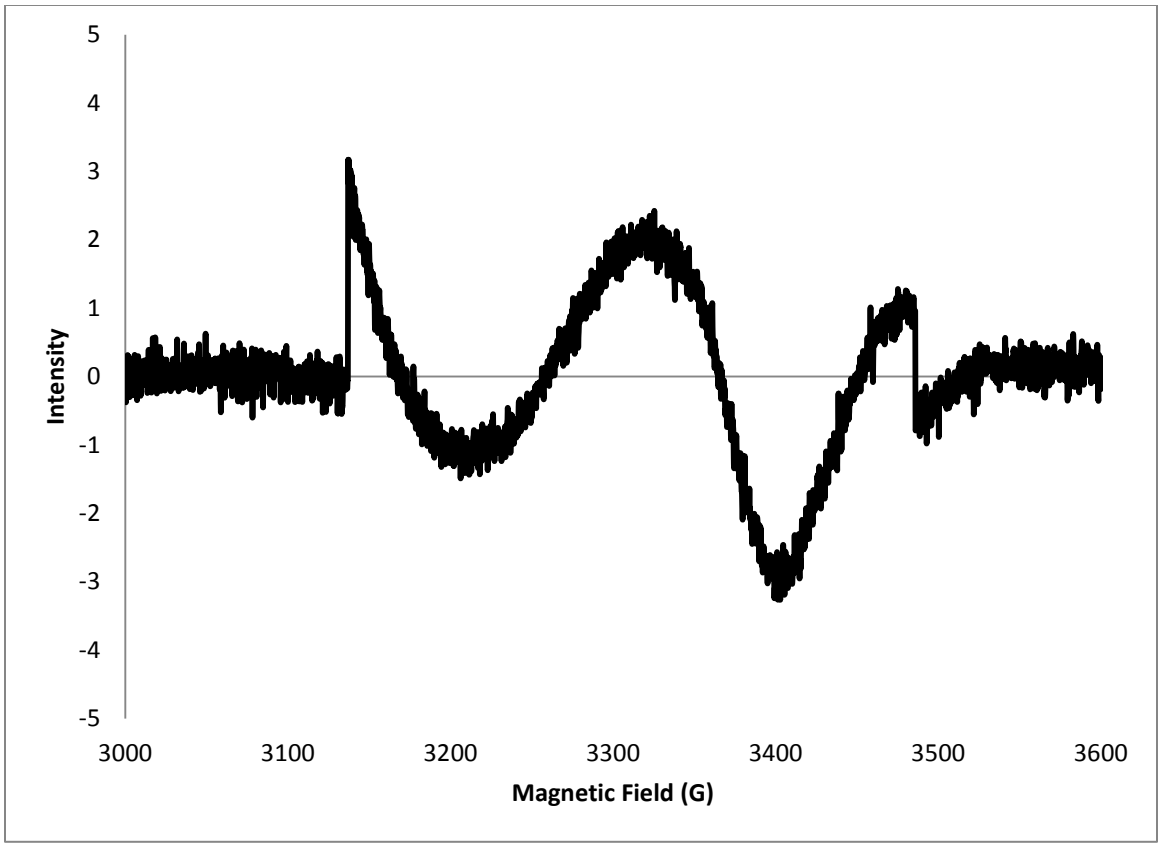

Figure 42 – EPR spectrum of copper coordination polymer obtained at room temperature.

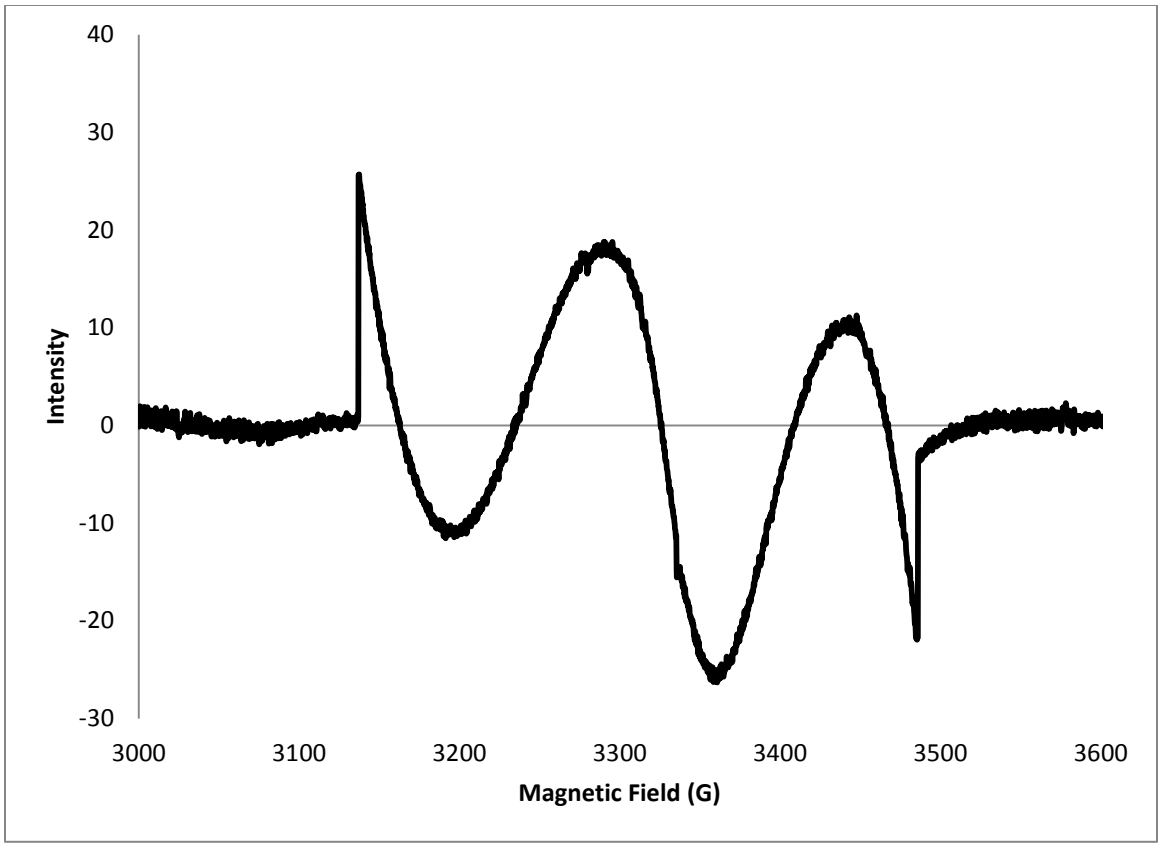

Figure 43 – EPR spectrum of copper coordination polymer obtained at 77 K.

The EPR spectrum of the iron coordination polymers can be seen in Figure 38, and as expected do not display any signals. This is because the metal centre of this compound possesses six electrons, and as a result contains no unpaired electrons. The EPR spectrum of the copper coordination polymer however is much more interesting.

The copper centre of copper coordination polymer is a d^9 complex, and therefore contains an unpaired electron. This unpaired electron results in a significant EPR signal, and its effect can also be seen in the ^1H NMR spectrum of the polymer (Figure 33). The EPR spectra of the copper coordination polymer can be seen in Figures 40 and 42, which display an intensity plot averaged over many scans and a single scan, respectively. It

must be noted however, that the averaged spectrum, Figure 40, displays signals not caused by the copper coordination polymer. This is due to the fact that the large, broad peak from 2000 to 3000 G is actually the result of a signal caused by the quartz tube in which the sample was measured, as can be seen in Figure 41.

The signal seen in Figure 42 shows the characteristic spectrum caused by a compound with a rhombic magnetic moment.[70] This is expected, as octahedral compounds experience a rhombic distortion of the magnetic moment.[106] The interaction with a magnetic nucleus experienced by an electron in a radical compound is generally much lower than that of the heavier nuclei in paramagnetic transition metal complexes, and not present in EPR spectra. Because this complex is a paramagnetic transition metal, it would be expected that signals caused by the nuclear hyperfine coupling of the electron with the copper nucleus would be present. More specifically, because both ^{63}Cu and ^{65}Cu possess a spin of 3/2, it would be expected that a "quartet" signal of low intensity would be present.[71] Unfortunately, this signal would occur before the main signal at 3300G, and as a result is obscured by the interference caused by the quartz tube.

EPR spectra of both the iron and copper coordination polymers were also obtained at 77 K, and can be seen in Figures 39 and 43, respectively. The iron coordination polymer displays no change and still shows no paramagnetic behaviour at low temperatures, as expected. The copper coordination polymer, however, does display a difference at low temperatures with the intensity of the signal increasing by nearly an order of magnitude and an increase in the splitting of the signal. This is expected for a low temperature EPR spectrum as the decreased temperature causes an increase in the population electrons occupying the lower energy magnetic moment.

4 - Experimental

4.1 – Materials

All reagents and solvents were obtained from Sigma Aldrich or Fisher and used without further purification.

4.2 – Instrumentation

NMR experiments were performed on a Bruker Avance 300 NMR using Topspin 1.3 software. IR spectra were obtained on a Bruker Alpha-p FTIR. Data used for fluorescence analysis was obtained on a Varian Cary 50 Bio Absorbance spectrometer and a Horiba Scientific PTI QM-400 fluorimeter. XRD measurements were performed on a Bruker axs D8 Advance instrument and EPR experiments were performed on an Active Spectrum Micro ESR. Thermogravimetric analysis was performed on a TA Instruments TGA Q500 and differential scanning calorimetry was performed on a TA Instruments DSC Q100.

4.3 – Synthesis

4.3.1 – 1,5-Bis(2`-pyridyl)pentane-1,3,5-trione (1)[54]

Sodium hydride (60% dispersion in mineral oil, 5.03 g, 125 mmol) in 1,2-dimethoxy ethane (50 mL) was stirred under a nitrogen atmosphere. To this suspension was added a solution of acetone (1.82 mL, 25 mmol) and ethyl-2-picolinate (10.09 mL, 75 mmol) in 1,2-dimethoxy ethane (50mL). This mixture was allowed to stir at room

temperature until a violent reaction occurred resulting in a bright orange suspension (variable time). This suspension was then heated to reflux for 6 hours and the solvent was then removed *in vacuo* yielding a brown paste. Water (100 mL) was added to this paste, and the resulting orange solution was filtered through Celite. Hydrochloric acid (1 M) was added dropwise to adjust the pH to 7, yielding a yellow precipitate which was collected by vacuum filtration. The product was then dissolved in chloroform and dried over magnesium sulphate. The solvent was removed *in vacuo* and the product was obtained as a flaky, yellow solid (**1**) (4.33 g, 63.1%). The ^{1}H NMR spectrum was identical to those reported in the literature.[54]

4.3.2 – 4`-Hydroxy-2,2`:6`,2``-terpyridine (2)[54]

Compound **1** (2.09 g, 8 mmol) and ammonium acetate (4.4 g, excess) were dissolved in ethanol (50 mL), resulting in a dark brown solution which was then heated to reflux for 6 hours. Solvent was removed *in vacuo* to reduce the solution to half volume, and the solution was then cooled in a refrigerator for 18 hours. The resulting precipitate was then collected by vacuum filtration and dried, yielding an off-white, crystalline product (**2**) (1.21 g, 58.4%). The ^{1}H NMR spectrum was identical to those reported in the literature.

4.3.3 – 4`-Chloro-2,2`:6`,2``-terpyridine (3)[54]

Compound **2** (1.0 g, 4 mmol) and phosphorous pentachloride (2.11 g, 10 mmol) were dissolved in phosphorous oxychloride (50 mL) and the resulting solution was heated to reflux for 12 hours. The solvent was then cautiously removed *in vacuo* and the resulting solid was dissolved in water (50 mL). This yielded an extremely acidic solution which was then made basic by the addition of solid potassium hydroxide which caused

the formation of a white precipitate. This precipitate was extracted with chloroform (3 × 15 mL) and dried over magnesium sulphate. The solvent was then removed *in vacuo* and the product was obtained as a light grey solid (**3**) (0.67 g, 62.1 %). The ^{1}H NMR spectrum was identical to those reported in the literature.[54]

4.3.4 – Disubstituted thiobisbenzenethiol-terpyridine monomer (4)

Compound **3** (0.43 g, 1.6 mmol) and thiobisbenzenethiol (0.20 g 0.8 mmol) were dissolved in dimethylformamide (20 mL) and stirred under nitrogen atmosphere for 10 minutes. After this, the solution was allowed to sit without stirring under a constant flow of nitrogen for 24 hours. The solution was then precipitated by dropwise addition into diethyl ether (400 mL) and the resulting bright yellow precipitate was collected by vacuum filtration yielding the product as a yellow-brown solid (**4**) (0.45 g, 78.8%). ^{1}H NMR (300 MHz, DMSO-d_6) δ (ppm) 8.69 (m, 8H), 8.20 (s, 4H), 8.10 (ddd, J = 7.8, 1.6 Hz, 4H), 7.70 (d, 4H), 7.58 – 7.52 (m, 4H). ^{13}C NMR (75 MHz, DMSO-d_6) δ (ppm) 154.0, 153.1, 151.5, 148.4, 139.0, 136.5, 135.5, 132.2, 128.5, 125.2, 121.8, 118.3. HSQC (DMSO-d_6) δ (ppm) 8.69 ↔ 148.4, 8.69 ↔ 121.8, 8.20 ↔ 118.3, 8.10 ↔ 139.0, 7.70 ↔ 135.5, 7.55 ↔ 132.3, 7.55 ↔ 125.2.

4.3.5 – Iron Polymer (5)

Compound **4** (0.051 g, 0.07 mmol) and $FeCl_2$ (0.009 g, 0.07 mmol) were dissolved in a minimum amount of dimethylformamide (approximately 1.5 mL) resulting in the instantaneous formation of a vibrant, deep purple solution. This solution was stirred under a nitrogen atmosphere for 3 hours after which an excess of ammonium hexafluorophosphate (0.05 g, 0.28 mmol) was added. The solution was then precipitated by dropwise addition into diethyl ether (300 mL) and cooled in a freezer. The bright

purple precipitate was then collected by vacuum filtration yielding the product as a dark purple powder (0.059 g, 69.6%). ^{1}H NMR (300 MHz, DMSO-d_6) δ (ppm) 9.03 (s), 8.66 (s), 7.92 (s), 7.83 (s), 7.68 (s), 7.14 (s), 6.98 (s).

4.3.6 – Cobalt Polymer (6)

Compound **4** (0.02 g, 0.028 mmol) and $Co(OAc)_2 \cdot 4 H_2O$ (0.007 g, 0.028 mmol) were dissolved in a minimum amount of dimethylformamide (approximately 1 mL) and were then heated to 80°C and stirred under a nitrogen atmosphere for 3 hours resulting in a brilliant turquoise solution. An excess of ammonium hexafluorophosphate (0.018 g, 0.11 mmol) was then added and the solution was precipitated by dropwise addition into diethyl ether (400 mL) and the precipitate was collected by vacuum filtration yielding a light turquoise powder (0.015 g, 53.2%).

4.3.7 – Nickel Polymer (7)

Compound **4** (0.02 g, 0.028mmol) and $Ni(OAc)_2 \cdot 4 H_2O$ (0.007 g, 0.028 mmol) were dissolved in a minimum amount of dimethylformamide (approximately 1 mL) and were then heated to 80°C and stirred under a nitrogen atmosphere for 12 hours resulting in an olive green solution. An excess of ammonium hexafluorophosphate (0.018 g, 0.11 mmol) was then added and the solution was precipitated by dropwise addition into diethyl ether (400 mL) and the precipitate was collected by vacuum filtration yielding a light green powder (0.012 g, 42.3%).

4.3.8 – Zinc Polymer (8)

Compound **4** (0.02 g, 0.028 mmol) and $Zn(OAc)_2$ (0.0051 g, 0.028 mmol) were dissolved in a minimum amount of dimethylformamide (approximately 1 mL) and were

then heated to 80°C for 12 hours. An excess of ammonium hexafluorophosphate (0.018 g, 0.11 mmol) was then added and the solution was precipitated by dropwise addition into diethyl ether (400 mL) and the precipitate was collected by vacuum filtration yielding a pale yellow powder (0.016 g, 57.4%).

4.3.9 – Copper Polymer (9)

Compound **4** (0.02 g, 0.028 mmol) and $Cu(OAc)_2 \cdot 1\ H_2O$ (0.0056 g, 0.028 mmol) were dissolved in a minimum amount of dimethylformamide (approximately 1 mL) and were heated to 80°C for 12 hours. An excess of ammonium hexafluorophosphate (0.018 g, 0.11 mmol) was then added and the solution was precipitated by dropwise addition into diethyl ether (400 mL) and the precipitate was collected by vacuum filtration yielding a pastel green powder (0.013 g, 46.8%).

4.3.10 – Ruthenium Polymer (10)

Compound **4** (0.015 g, 0.02 mmol) and $RuCl_3$ (0.0087 g, 0.04 mmol) were dissolved in a minimum amount of dimethylformamide (approximately 1 mL) and were then heated at 80°C for 4 hours. A second equivalent of compound 4 (0.015 g, 0.02 mmol) and three drops of 4-ethylmorpholine were then added and the solution was heated at 80°C for another 4 hours. An excess of ammonium hexafluorophosphate (0.027 g, 0.17 mmol) was then added and the solution was precipitated by dropwise addition into diethyl ether (400 mL) and the precipitate was collected by vacuum filtration yielding the product as a deep red powder (0.021 g, 45.2%).

5 – Conclusions and Future Work

A novel, bis-terpyridine ligand was synthesized, and from this a novel, highly conjugated iron coordination polymer was prepared. This deep purple compound was characterized using NMR spectroscopy, and its thermal properties were examined using TGA and DSC. It was unfortunately not a viable candidate for GPC, and its molecular weight was instead determined using viscometry measurements. This molecular weight is estimated to be approximately 40,000 g/mol, corresponding to a chain length of approximately 36 monomeric units. The polymer was unfortunately not found to exhibit conductive properties resulting from the doping techniques performed.

The terpyridine monomer was then used to prepare a series of coordination polymers from several transition metals, including nickel, zinc, cobalt, copper, and ruthenium. These polymers were analysed using ^{1}H NMR spectroscopy and EPR spectroscopy. They were also examined using fluorescence spectroscopy, and it was found that the zinc coordination polymer exhibited a fluorescence enhancement of approximately five times the intensity over the monomer, while the other polymers analysed displayed the expected fluorescent quenching. The solvent effects on the fluorescence of the zinc coordination polymer were examined, and the polymer was determined to have a fluorescent quantum yield of 3.3×10^{-3}.

One important focus of future work will be attempts to find an appropriate doping method in order to produce conductivity in the iron coordination polymer. This may be performed through trials of other gentle doping techniques or through more aggressive doping techniques on the monomer before polymerization.

Extensive characterization should also be performed on the remaining polymers in the transition metal coordination series. This may include thermal analysis such as TGA and DSC as well as viscometric measurements in order to estimate the molecular weights of the polymers.

References

[1] He, C.; Liu, D.; Lin, W. *Chem. Rev.*, **2015**, *115*, 11079-11108.

[2] Kaur, R.; Kim, K. H.; Paul, A. K.; Deep, A. *J. Mater. Chem. A*, **2016**, *4*, 3991-4002.

[3]Stahl, G. E. *Experimenta, Observationes, Animadversiones* CCC Numero, Chymicae et Physicae, Berlin, **1731**, pp. 281–283.

[4] Weiser H. B.; Milligan, W. O.; Bates, J. B. X-Ray Diffraction Studies on Heavy-metal Iron-cyanides. *J. Phys. Chem.*, **1942**, *46* (1), 99-111.

[5] Piernas-Muñoz, M. J.; Castillo-Martínez, E.; Roddatis, V.; Armand, M.; Rojo, T. *J. Power Sources*, **2014**, *271*, 489-496.

[6] West, C. D. *Z. Kristallogr*., **1935**, *90*, 555.

[7] Jensen, K. A. *Z. Anorg. Chem.*, **1944**, *252*, 227.

[8] Martin, K. V.; Judd, M. L. Report on contract AF 33(616) 3200 (Nov. 1956) to U.S. Air Force, Wright Air Development Center, Final Report on Contract AF 33(616) 3772 (Dec. 1957).

[9] Kealy, T. J.; Pauson, P. L. *Nature*, **1951**, *168*, 1039.

[10] Wilkinson, G.; Rosenblum, M.; Whiting, H. C.; Woodward, R. B. *J. Am. Chem. Soc*. **1952**, *74*, 2125.

[11] Wells, A. F. *Structural Inorganic Chemistry, 5th ed.*, Oxford University Press, Oxford, **1984**.

[12] Wells, A. F. *Three Dimensional Nets and Polyhedra*, Wiley, New York, **1977**.

[13] Robson, R.; Abrahams, B. F.; Batten, S. R.; Gable, R. W.; Hoskins, B. F.; Liu, J. P. *ACS Symp. Ser.*, **1992**, *499*, 256.

[14] Batten, S. R.; Neville, S. M.; Turner, D. R. *Coordination Polymers: Design, Analysis and Application*, RSC, Cambridge, **2009**.

[15] IUPAC. *Nomenclature of Inorganic Chemistry, IUPAC Recommendations 2005*. Connelly, N.; Damhus, T.; Harshorn, R. M. Eds., RCS, Cambridge, **2005**.

[16] Batten, S. R.; Champness, N. R.; Chen, X.; Garcia-Martinez, J.; Kitagawa, S.; Öhrström, L.; O'Keeffe, M.; Suh, M. P.; Reedijk, *J. Pure. Appl. Chem*., **2013**, *85*, 1715-1724

[17] Bailor, J. C. in *Organometallic Polymers,* Carraher, C.; Sheats, J.; Pittman, C. Eds., Organometallic Polymers, Academic Press, New York, **1978**.

[18] Janiak, C. *Dalton Trans.*, **2003**, 2781-2804

[19] Hofmeir, H.; Schubert, U. S. *Chem. Soc. Rev.*, **2004**, 33, 373-399.

[20] Cheng, P. Y.; Chen, C. Y.; Lee, H. M. *Inorg. Chim. Acta.*, **2009**, *362*, 1840-1846.

[21] Xiao, B.; Hou, H.; Fan, Y. *J. Mol. Catal. A. – Chem.*, **2008**, *288*, 42-51.

[22] Chen, C. Y.; Cheng, P. Y.; Wu, H. H.; Lee, H. M. *Inorg. Chem.*, **2007**, *46*, 5691-5699.

[23] Roesky, H. W.; Andruh, M. *Coord. Chem. Rev.*, **2003**, *236*, 91-119.

[24] Tranchemontagne, D. J.; Mendoza-Cortez, J. L.; O'Keeffe, M.; Yaghi, O. M. *Chem. Soc. Rev.*, **2009**, *38*, 1257.

[25] Pan, L.; Olson, D. H.; Ciemnolonski, L. R.; Heddy, R.; Li, J. *Angew. Chem., Int. Ed.*, **2006**, *45*, 616.

[26] Yang, Y.; Hu, Q.; Zhang, Q.; Jiang, K.; Lin, W.; Yang, Y.; Cui, Y.; Qian, G. *Mol. Pharmaceutics*., **2016**, *13*, 2782-2786.

[27] Cametti, M.; Martí-Rujas, J. *Dalton Trans.*, **2016**, *45*, 18832-18837.

[28] Chen, Y. A.; Tsai, F. J.; Zeng, Y. T.; Wang, J. C.; Hong, C. P.; Huang, P. H.; Chuang, H. L.; Lin, S. Y.; Chan, C. T.; Ko, Y. C.; Chou, Y. C.; Lin, T. L.; Lee, G. H.; Ho, M. L. *J. Chin. Chem. Soc*., **2016**, *63*, 424-431.

[29] Mak, C. S. K.; Leung, Q. Y.; Li, C. H.; Chan, W. K.. *J. Polym. Sci. A*, **2010**, *48*, 2311-2319.

[30] Chien, C. H.; Liaoo, S. F.; Wu, C. H.; Shu, C. F.; Chang, S. Y.; Chi, Y. *Adv. Funct. Mater.*, **2008**, *18*, 1430-1439.

[31] Efremova, O. A.; Brylev, K. A.; White, M. S.; Shestopalov, M. A.; Kitamura, N.; Mironov, Y. V.; Bauer, S.; Sutherland, A. J. *J. Mater. Chem. C*, **2014**, *2*, 8630-8638.

[32] Ward, M. D. *Chem. Soc. Rev.*, **1995**, 121-134

[33] Grozema, F. C.; Siebbeles, L. D. A. *Charge and Exciton Transport through Molecular Wires*, Siebbeles, L. D. A.; Grozema, F. C. Eds., Wiley, Weinheim, **2011**.

[34] Arrhenius, T. S.; Blanchard-Desce, M.; Dvolaitzky, M.; Lehn, J. M. *Proc. Natl. Acad. Sci. USA*, **1986**, *83*, 5355-5359.

[35] Vrbanić, D.; Remškar, M.; Jesih, A.; Mrzel, A.; Umek, P.; Ponikvar, M.; Jančar, B.; Meden, A.; Novosel, B.; Pejovnik, S.; Venturini, P.; Coleman, J. C.; Mihailović, D. *Nanotechnology*, **2004**, *15*, 635-638.

[36] Winters, M. U.; Karnbratt, J.; Eng, M.; Wilson, C. J.; Anderson, H. L.; Albinsson, B. *J. Phys. Chem. C*, **2007**, *111*, 7192-7199.

[37] El-Ghayoury, A.; Schenning, A. P. H. J.; Van Hal, P. A.; Van Duren, J. K. J.; Jansen, R. A. J.; Meijer, E. W. *Angew. Chem. Int. Ed. Engl.*, **2001**, *40*, 3660-3663.

[38] Cacilli, F.; Wilson, J. S.; Michels, J. J.; Daniel, C.; Silva, C.; Friend, R. H.; Severin, N.; Samori, P.; Rabe, J. P.; O'Connel, M. J.; Taylor, P. N.; Anderson, H. L. *Nat. Mater.*, **2002**, *1*, 160-164.

[39] Dai, L. *Intelligent Macromolecules for Smart Devices: From Materials Synthesis to Device Applications*, Springer, London, **2004**.

[40] Akamatu, H.; Inokutchi, H.; Matsunaga, Y. *Nature*, **1954**, *173*, 168.

[41] Wright, P. V. *Br. Polym. J.*, **1975**, *7*, 319.

[42] Hendy, B. N. *Ionic Polymers*, in *Specialty Polymers*, Dyson, R. W. Ed. Springer US, Boston, Ma., **1987**.

[43] Shirakawa, H.; Louis, E. L.; MacDiarmid, A. G. *J. Chem. Soc. Chem. Commun.*, **1997**, 578.

[44] Yamamoto, T.; Sanechika, K.; Yamamoto, A. *J. Polym. Sci., Polym. Lett. Ed.*, **1980**, *18*, 9-12.

[45] Diaz, A.; Kanazawa, K.; Gardini, G. *J. Chem. Soc: Chem. Commun.*, **1979**, 635-636.

[46] Diaz, A. F.; Logan, J. A. *J. Electroanal. Chem.*, **1980**, *111*, 111-114.

[47] Harrison, W. A. *Solid State Theory*, Dover, New York, **1979**.

[48] Wikimedia Commons. https://commons.wikimedia.org/wiki/File:Band_filling_diagram.svg (accessed March 14, 2017).

[49] Brédas, J. L.; Street, G. B. *Acc. Chem. Res.*, **1985**, *18*, 309-315.

[50] Burroughes, J. H.; Bradley, D. D. C.; Brown, A. R.; Marks, R. N.; Mackay, K.; Friend, R. H.; Holmes, A. B. *Nature*, **1990**, *347*, 539-541.

[51] Yu, G.; Gao, J.; Hummelen, J. C.; Wudl, F.; Heeger, J. *Science*, **1995**, *270*, 1789-1791.

[52] Morgan, G. T.; Burstall, F. H. *J. Chem. Soc., Abstr.*, **1932**, 20-30.

[53] Constable, E. C. *Adv. Inorg. Chem. Radiochem.*, **1986**, *30*, 69.

[54] Constable, E. C.; Ward, M. D. *J. Chem. Soc. Dalton Trans.*, **1990**, 1405.

[55] Constable, E. C.; Thompson, A. M. W. C. *New J. Chem.*, **1992**, *16*, 855-876

[56] Constable, E. C.; Lewis, J.; Liptrot, M. C.; Raithby, P. R. *Inorg. Chim. Acta.*, **1990**, *178*, 47-54.

[57] Constable, E. C.; Thompson, A. M. W. C.; Armaroli, N.; Balzani, V.; Maestri, M. *Polyhedron*, **1992**, *11*, 2707-2709

[58] Hanan, G. S.; Volkmer, D.; Schubert, U. S.; Lehn, J. M.; Baum, G.; Fenske, D. *Angew. Chem., Int. Ed.*, **1997**, *36*, 1842-1844.

[59] Hanan, G. S.; Schubert, U. S.; Volkmer, D.; Rivière, E.; Lehn, J. M.; Kyritsakas, N.; Fischer, J. *Can. J. Chem.*, **1997**, *75*, 169-182.

[60] Schubert, U. S.; Eschbaumer, C. *J. Inclusion Phenom. Macrocyclic Chem.*, **1999**, *35*, 101-109.

[61] Constable, E. C.; Thompson, A. M. W. C. *J. Chem. Soc., Chem. Commun.*, **1992**, 617-619.

[62] Constable, E. C.; Thompson, A. M. W. C. *J. Chem. Soc. Dalton Trans.*, **1992**, 3467-3475.

[63] Abd-El-Aziz, A. S.; Dalgakiran, S.; Vandel, M.; Owen, E. M.; Wagner, B. D. *J. Electrochem Soc.*, **2013**, *160*, G61-G67

[64] Zhao, M.; Tan, J.; Su, J.; Zhang, J.; Zhang, S.; Wu, J.; Tian, Y. *Dyes Pigm.*, **2016**, *130*, 216-225.

[65] Wang, J.; Yuan, F.; Hu, H. M.; Bai, C.; Xue, G. L. *Innorg. Chem. Comm.*, **2016**, *73*, 37-40.

[66] Chakraborty, C.; Pandey, R. K.; Hossain, Md. D.; Futera, Z.; Moriyama, S.; Higuchi, M. *ACS Appl. Mater. Interfaces*, **2015**, *7*, 19034-19042.

[67] Carter, K. P.; Zulato, C. H. F.; Rodrigues, E. M.; Pope, S. J. A.; Sigola, F. A.; Cahill, C. L. *Dalton Trans.*, **2015**, *44*, 15843-15854.

[68] Silverstein, R. M.; Webster, F. X.; Kiemle, D. J. *Spectrometric Identification of Organic Compounds*, Wiley, Hoboken, NJ, **2005**.

[69] Solomons, T. W. G.; Fryhle, C. B. *Organic Chemistry*, Wiley, Hoboken, NJ, **2008**.

[70] Palmer, G. *Meth. Enzymol.*, **1967**, *10*, 594-609.

[71] DeRose, V. J.; Hoffman, B. M. *Meth. Enzymol.*, **1995**, *246*, 554-589.

[72] Chiesa, M.; Giamello, E.; Che, M. *Chem. Rev.*, **2010**, *110*, 1320-1347.

[73] Coats, A. W.; Redfern, J. P. *Analyst*, **1963**, *88*, 906-924

[74] O'Neill, M. J. *Anal. Chem.*, **1964**, *36*, 1238-1245.

[75] Bissessur, R. Fluorescence Spectroscopy: Lecture #8

[76] Lakowicz, J. R. *Principles of Fluorescene Spectroscopy*, Springer, Baltimore, MD, **2006**.

[77] Harris, D. C. *Quantitative Chemical Analysis, 7th Ed.*, W. H. Freeman and Company, New York, **2007**.

[78] Hofmeier, H.; Schmatloch, S.; Wouters, D.; Schubert, U. S. *Macromol. Chem. Phys.*, **2003**, *204*, 2197-2203.

[79] Strekowski, L.; Majosn, C. J.; Lee, H.; Gupta, R.; Sowell, J.; Patonay, G. *J. Heterocyclic. Chem.*, **2003**, *40*, 913.

[80] Kornblum, N.; Ackerman, P.; Manthey, J. W.; Musser, M. T.; Pinnick, H. W.; Singaram, S.; Wade, P. A. *J. Org. Chem.*, **1988**, *53*, 1475-1481.

[81] Russell, G. A.; Pecoraro, J. M. *J. Am. Chem. Soc.*, **1979**, *101*, 3331-3334.

[82] Prousek, J. *Collect. Czech. Chem. Commun.*, **1988**, *24*, 1013-1018.

[83] Wu, K.; Dolbier, W. R. Jr.; Battiste, M. A.; Zhai, Y. *Mendeleev. Commun.*, **2006**, *16*, 146-147.

[84] Zhou, D. Y.; Dou, H. Y.; Zhao, C. Z.; Chen, Q. Y. *J. Fluorine Chem.*, **2006**, *127*, 740-745.

[85] Strekowski, L.; Lipowska, M.; Patonay, G. *J. Org. Chem.*, **1992**, *57*, 4578-4580.

[86] Bunnett, J. F. *Acc. Chem. Res.*, **1978**, *11*, 413.

[87] Kornblum, N.; Michel, R. E.; Kerber, R. C. *J. Am. Chem. Soc.*, **1966**, *88*, 5662.

[88] Constable, E. C. *J. Chem. Soc. Dalton Trans.*, **1985**, 2687-2689.

[89] Schmatloch, S.; van den Berg, A. M. J.; Alexeev, A. S.; Hofmeier, H.; Schubert, U. S. *Macromolecules*, **2003**, *36*, 9943-9949.

[90] Hofmeier, H.; Hoogenboom, R.; Wouters, M. E. L.; Schubert, U. S. *J. Am. Chem. Soc.*, **2005**, 2913-2921.

[91] Russo, P. S.; Saunders, M. J.; Karasz, F. E. *Macromolecules*, **1986**, *19*, 2856-2859.

[92] Russo, P. S., Georgia Institute of Technology, Atlanta, Georgia, *Intrinsic Viscosity*, **2008**.

[93] American Polymer Standards Corporation, *Mark-Houwink Parameters for Polymers*, http://www.ampolymer.com/Mark-HouwinkParameters.html (accessed Feb 13, 2017)

[94] Chisholm, M. H.; Hadad, C. M.; Heinze, K.; Hempel, K.; Singh, N.; Vyas, S. *J. Clust. Sci.*, **2008**, *19*, 209.

[95] Kuehl, C. J.; Da Re, R. E.; Scott, B. L.; Morris, D. E.; John, K. D. *Chem. Commun.*, **2003**, 2336-2337.

[96] Kar, P. *Doping in Conjugated Polymers*, John Wiley and Sons, Hoboken, NJ, **2013**.

[97] Chourasia, A. B.; Kelkar, D. S. *AIP Conf. Proc.*, **2013**, 911.

[98] Duncan, J. F.; Mok, K. F. *Aust. J. Chem.*, **1966**, *19*, 701-703.

[99] Adeloye, A. O.; Olomola, T. O.; Adebayo, A. I.; Ajibade, P. A. *Int. J. Mol. Sci.*, **2012**, *13*, 3511-3526.

[100] Schubert, U. S.; Eschbaumer, C.; Andres, P.; Hofmeier, H.; Weidl, C. H.; Herdtweck, E.; Dulkeith, E.; Morteani, A.; Hecker, N. E.; Feldmann, *J. Synth. Met.*, **2001**, *121*, 1249-1252.

[101] Chow, H. S.; Constable, E. C.; Housecroft, C. E.; Neuburger, M.; Schaffner, S. *Dalton Trans.*, **2006**, 2881-2890.

[102] Sun, W.; Wu, N.; Wang, W.; Kong, L.; Wu, J.; Li, S.; Tian, Y. *Dyes Pigm.*, **2016**, *133*, 86-92.

[103] Wang, H.; Tian, X.; Du, W.; Zhang, Q.; Guan, L.; Wang, A.; Zhang, Y.; Wang, C.; Zhou, H.; Wu, J.; Tian, Y. *J. Mater. Chem., B.*, **2016**, *4*, 4818.

[104] "Physical Constants of Organic Compounds," in *CRC Handbook of Chemistry and Physics, 97th Edition*, (Internet Version **2017**), W. M. Haynes, ed., CRC Press/Taylor & Francis, Boca Raton, FL.

[105] "Physical Constants of Organic Compounds," in *CRC Handbook of Chemistry and Physics, 97th Edition*, (Internet Version **2017**), W. M. Haynes, ed., CRC Press/Taylor & Francis, Boca Raton, FL.

[106] Salmeen, I.; Palmer, G. *J. Chem. Phys.*, **1968**, *48*, 2049-2052.